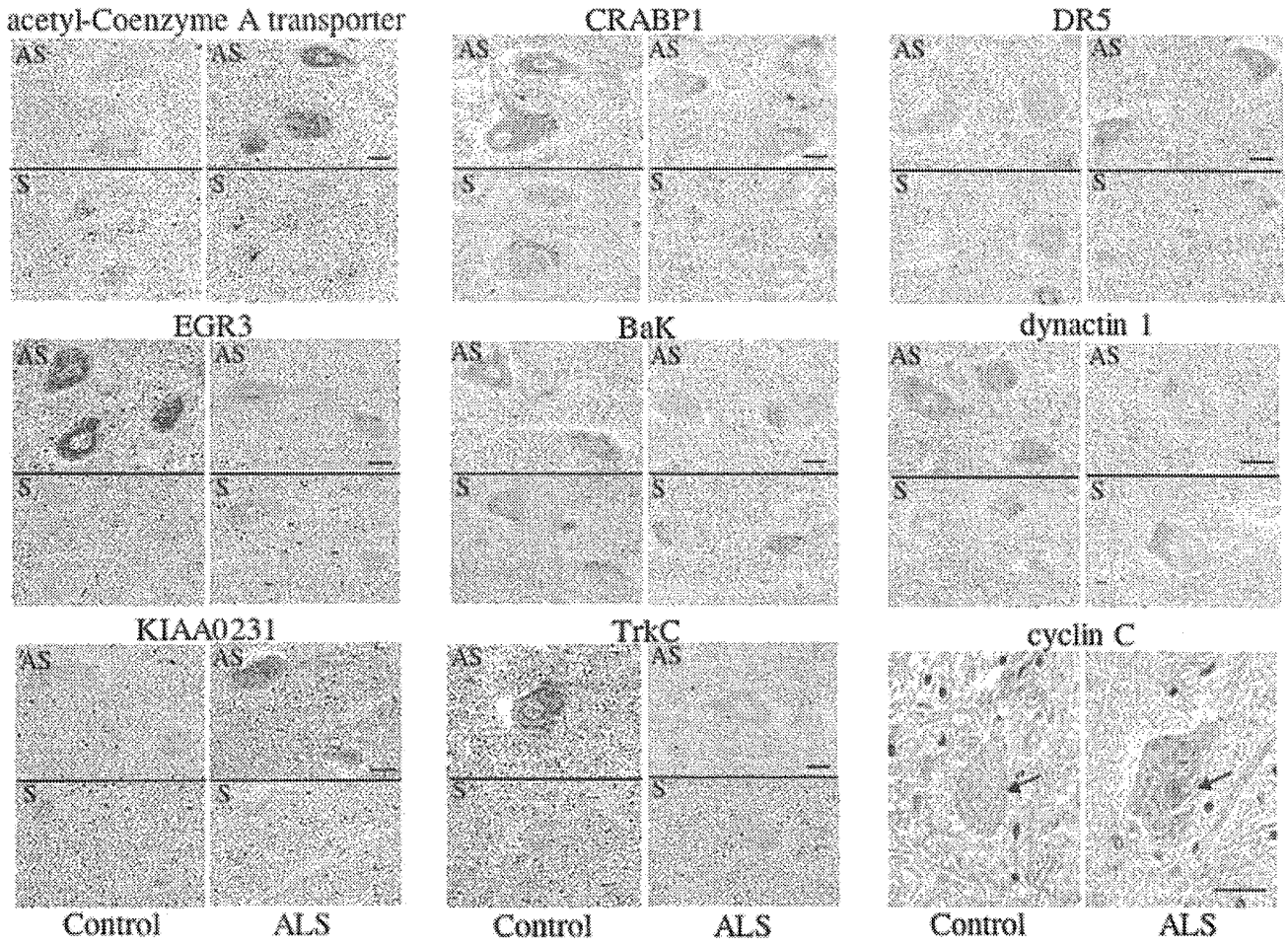

Fig 4. In situ hybridization and immunohistochemistry of the selected genes. Representative in situ hybridization is shown for acetyl-COENZYMEA transporter, EGR3, KIAA0231, CRABP1, Bak, TrkC, DR5, and dynactin 1. The antisense probe (AS) detects positive signals for the expression of each gene in spinal motor neurons for ALS and/or controls, but the sense probe (S) does not. Lipofuscin granules are seen as yellowish granules. Immunohistochemistry was preformed for cyclin C, and nuclear staining was prominent in ALS motor neurons. Arrows denote the nuclei. Bars = 25μm.

might be impaired in the neurodegenerative process of ALS. Among the genes related to transcriptional regulation, the number of significantly downregulated genes was twofold greater than that of the upregulated ones in ALS motor neurons. These downregulated transcription-related genes were not restricted to genes regulating neuronal differentiation as neuron-specific cellular properties, but also included genes such as RNA polymerase and transcription factors, which regulate general cellular functions. These observations suggest that downregulation of transcriptional activity may be the reflection of motor neuron dysfunction because of a wide range of impairments of cellular maintenance systems.

Interestingly, the expression of dynactin 1, which recently has been identified as a causative gene for human motor neuron disease,[42] was reduced in ALS motor neurons. Some other motor proteins including the kinesin family responsible for antegrade axonal transport and dyneins for retrograde axonal transport were not changed significantly, but the expression levels of MAPs 1A, 4, and tau were decreased, shown by their classification in SOM1 and SOM6. The impairment of axonal transport is thought to be an early event of motor neuron degeneration, and especially the protein levels of MAPs 1A and tau have been reported to decrease early before the onset of symptoms in mutant SOD1 transgenic mice.[43–45] The upregulation of ubiquitin-specific protease 11 (USP11), listed in Tables 2 and 3, also may be related to microtubule abnormality because the RanGTP-associated protein RanBPM, which is required for correct nucleation of microtubules, is the enzymatic substrate for USP11.[46] The present results imply that retrograde axonal transport, especially that associated with dynactin, might be affected even at the terminal stage of ALS and be crucial for motor neurons, although cytoskeletal proteins are the major functional group in the downregulated genes.

As for the death signals and inflammatory factors, we previously have reported that these genes were significantly upregulated in the spinal cord of mutant SOD1 transgenic mice,[15,17] suggesting that these inflammatory and apoptotic death signals play a crucial role in concert with motor neuron degeneration and inflammatory cellular reactions, including microglial activation.[7,47] However, in sporadic ALS spinal cords, the expression profiles of inflammation- and death signal–related genes are somewhat different from those in the Tg mouse model. Death receptor 5 (TNF receptor 10b, TNFR10b), TNF receptor–associated factor 6 (TRAF 6), interleukin-1 receptor antagonist, and ephrin A1 were overexpressed in ALS motor neurons, whereas the expression levels of the respective ligands or inducers, TNF-α, TNF superfamily member 10 (TRAIL) and IL-1β, were not markedly changed in either motor neurons or ventral horn homogenates. Because TNF-α was prominently upregulated in the Tg mouse spinal cords,[17] its almost unchanged expression level in sporadic ALS was a surprising observation. Many other inflammation-related genes were also not significantly upregulated in human ALS spinal cords, in contrast with the findings in animal models. Far less invasion and activation of microglia, a major source of TNF-α, IL-1β, and many other inflammatory factors, were seen in human ALS spinal cords at the terminal autopsy stage as compared with those of Tg mice,[48] which could explain these differences.

Genes related to apoptotic pathways, caspase-1, -3, -9, caspase, and RIP adaptor with death domain (CRADD), were upregulated in ALS motor neurons in SOM analysis (SOM24 and SOM25), and an antiapoptotic factor, NF-κB, was markedly upregulated. Although Bax, a proapoptotic Bcl-2 family member, has been reported to increase in ALS motor neurons,[49,50] and another member, Bak, was underexpressed in this study, the expression of Bcl-2 and Bcl-xL, antiapoptotic Bcl-2 family members was not significantly altered in motor neurons, possibly suggesting that Bcl-2 family members are not primarily involved in motor neuron degeneration in sporadic ALS. Cyclin A1 and C were upregulated (SOM25) and cyclin E was downregulated (SOM1) in ALS motor neurons. These cell cycle regulators are specific to G1/S phase transition, and upregulation of these cyclins enhances arrest in G1/S phase, preventing entry into S phase. Our finding on cyclin expression support the recently reported view that G1/S phase is aberrantly activated in ALS motor neurons, eventually inducing motor neuron death.[51] The subcellular localization of cyclin C in the nucleus may trigger cell death signaling mechanisms. These factors related to the cell death signaling pathway, TNFR, TRAF6, CRADD, caspases, cyclins, Bak, and NF-κB may be involved in the motor neuron degeneration process in sporadic ALS, although we cannot simply state that an apoptotic process is present in ALS motor neurons, as has been suggested by many histological analyses.[6] Becausse neuronal cell degeneration and the eventual neuronal cell death process are the results of interactions of complex pathways involving many factors and signaling molecules, we need to further elucidate the pathophysiological significance of these factors with altered expression levels in ALS motor neurons.

Microarray analysis on the laser-captured motor neurons provided us with significant information about motor neuron degeneration and dysfunction in sporadic ALS patients. Such information cannot be obtained by whole spinal cord tissue microarray assay,[52] as discussed above. Although this study was performed on postmortem patients' tissues, the remaining individual motor neurons would express ongoing or even early molecular events in the neurodegeneration process, because motor neurons in the remaining motor neuron population randomly enter into the degeneration process among up to the terminal stage in ALS.[53] We need to study larger numbers of ALS patients, and to understand the pathophysiological roles of candidate genes identified by the combined methodology of DNA microarray analysis and LCM, compared with other neurodegeneration processes. This methodology provides crucial clues about candidate genes whose related products might hamper the disease process of ALS.

This work was supported by a Center of Excellence grant from the Ministry of Education, Culture, Sports, Science and Technology of Japan, and grants from the Ministry of Health, Labor and Welfare of Japan.

References

1. Ince PG, Lowe J, Shaw PJ. Amyotrophic lateral sclerosis: current issues in classification, pathogenesis and molecular pathology. Neuropathol Appl Neurobiol 1998;24:104–117.
2. Bunina TL. On intracellular inclusions in familial amyotrophic lateral sclerosis. Korsakov J Neuropath Psychiat 1962;62: 1293–1296.
3. Okamoto K, Hirai S, Amari M, et al. Bunina bodies in amyotrophic lateral sclerosi immunostained with rabbit anti-cystatin C serum. Neurosci Lett 1993;162:125–128.
4. Cleveland DW, Rothstein JD. From Charcot to Lou Gehrig: deciphering selective motor neuron death in ALS. Nat Rev Neurosci 2001;2:806–819.
5. Bergeron C. Oxidative stress: its role in the pathogenesis of amyotrophic lateral sclerosis. J Neurol Sci 1995;129(suppl): 81–84.
6. Sathasivam S, Ince PG, Shaw PJ. Apoptosis in amyotrophic lateral sclerosis: a review of the evidence. Neuropathol Appl Neurobiol 2001;27:257–274.
7. Hand CK, Rouleau GA. Familial amyotrophic lateral sclerosis. Muscle Nerve 2002;25:135–159.
8. Ishigaki S, Liang Y, Yamamoto M, et al. X-Linked inhibitor of apoptosis protein is involved in mutant SOD1-mediated neuronal degeneration. J Neurochem 2002;82:576–584.

9. Kawahara Y, Ito K, Sun H, et al. Glutamate receptors: RNA editing and death of motor neurons. Nature 2004;427:801.
10. Niwa J, Ishigaki S, Hishikawa N, et al. Dorfin ubiquitylates mutant SOD1 and prevents mutant SOD1-mediated neurotoxicity. J Biol Chem 2002;277:36793–36798.
11. Hishikawa N, Niwa J, Doyu M, et al. Dorfin localizes to the ubiquitylated inclusions in Parkinson's disease, dementia with Lewy bodies, multiple system atrophy, and amyotrophic lateral sclerosis. Am J Pathol 2003;163:609–619.
12. Luo J, Isaacs WB, Trent JM, Duggan DJ. Looking beyond morphology: cancer gene expression profiling using DNA microarrays. Cancer Invest 2003;21:937–949.
13. Alizadeh AA, Ross DT, Perou CM, van de Rijn M. Towards a novel classification of human malignancies based on gene expression patterns. J Pathol 2001;195:41–52.
14. Luo L, Salunga RC, Guo H, et al. Gene expression profiles of laser-captured adjacent neuronal subtypes. Nat Med 1999;5: 117–122.
15. Ando Y, Liang Y, Ishigaki S, et al. Caspase-1 and -3 mRNAs are differentially upregulated in motor neurons and glial cells in mutant SOD1 transgenic mouse spinal cord: a study using laser microdissection and real-time RT-PCR. Neurochem Res 2003; 28:839–846.
16. Ginsberg SD, Hemby SE, Lee VM, et al. Expression profile of transcripts in Alzheimer's disease tangle-bearing CA1 neurons. Ann Neurol 2000;48:77–87.
17. Yoshihara T, Ishigaki S, Yamamoto M, et al. Differential expression of inflammation- and apoptosis-related genes in spinal cords of a mutant SOD1 transgenic mouse model of familial amyotrophic lateral sclerosis. J Neurochem 2002;80:158–167.
18. Kamme F, Salunga R, Yu J, et al. Single-cell microarray analysis in hippocampus CA1: demonstration and validation of cellular heterogeneity. J Neurosci 2003;23:3607–3615.
19. Terao S, Sobue G, Hashizume Y, et al. Disease-specific patterns of neuronal loss in the spinal ventral horn in amyotrophic lateral sclerosis, multiple system atrophy and X-linked recessive bulbospinal neuronopathy, with special reference to the loss of small neurons in the intermediate zone. J Neurol 1994;241: 196–203.
20. Sobue G, Hashizume Y, Yasuda T, et al. Phosphorylated high molecular weight neurofilament protein in lower motor neurons in amyotrophic lateral sclerosis and other neurodegenerative diseases involving ventral horn cells. Acta Neuropathol (Berl) 1990;79:402–408.
21. Bohm M, Wieland I, Schutze K, Rubben H. Microbeam MOMeNT: non-contact laser microdissection of membrane-mounted native tissue. Am J Pathol 1997;151:63–67.
22. Watanabe H, Tanaka F, Doyu M, et al. Differential somatic CAG repeat instability in variable brain cell lineage in dentatorubral pallidoluysian atrophy (DRPLA): a laser-captured microdissection (LCM)-based analysis. Hum Genet 2000;107: 452–457.
23. Schutze K, Lahr G. Identification of expressed genes by laser-mediated manipulation of single cells. Nat Biotechnol 1998;16: 737–742.
24. Wang J, Delabie J, Aasheim H, et al. Clustering of the SOM easily reveals distinct gene expression patterns: results of a reanalysis of lymphoma study. BMC Bioinformatics 2002;3: 36–44.
25. Ross ME, Zhou X, Song G, et al. Classification of pediatric acute lymphoblastic leukemia by gene expression profiling. Blood 2003;102:2951–2959.
26. Malaspina A, Kaushik N, de Belleroche J. Differential expression of 14 genes in amyotrophic lateral sclerosis spinal cord detected using gridded cDNA arrays. J Neurochem 2001;77: 132–145.
27. Dangond F, Hwang D, Camelo S, et al. The molecular signature of late-stage human ALS revelated by expression profiling of post-mortem spinal cord gray matter. Physiol Genomics 2004;16:229–239.
28. Kanamori A, Nakayama J, Fukuda MN, et al. Expression cloning and characterization of a cDNA encoding a novel membrane protein required for the formation of *O*-acetylated ganglioside: a putative acetyl-CoA transporter. Pro Natl Acad Sci USA 1997;94:2897–2902.
29. Malisan F, Franchi L, Tomassini B, et al. Acetylation suppresses the proapoptotic activity of GD3 ganglioside. J Exp Med 2002; 196:1535–1541.
30. Rapport MM, Donnenfeld H, Brunner W, et al. Ganglioside patterns in amyotrophic lateral sclerosis brain regions. Ann Neuol 1985;18:60–67.
31. Chen HH, Tourtellotte WG, Frank E. Muscle spindle-derived neurotrophin 3 regulates synaptic connectivity between muscle sensory and motor neurons. J Neurosci 2002;22:3512–3519.
32. Mears SC, Frank E. Formation of specific monosynaptic connections between muscle spindle afferents and motoneurons in the mouse. J Neurosci 1997;17:3138–3135.
33. Yamamoto M, Sobue G, Yamamoto K, et al. Expression of glial cell line-derived neurotrophic factor mRNA in the spinal cord and muscle in amyotrophic lateral sclerosis. Neurosci Lett 1996; 204:117–120.
34. Zhou H, Muramatsu T, Halfter W, et al. A role of midkine in the development of the neuromuscular junction. Mol Cell Neurosci 1997;10:56–70.
35. Oosthuyse B, Moons L, Storkebaum E, et al. Deletion of the hypoxia-response element in the vascular endothelial growth factor promoter causes motor neuron degeneration. Nat Genet 2001;28:131–138.
36. Lambrechts D, Storkebaum E, Morimoto M, et al. VEGF is a modifier of amyotrophic lateral sclerosis in mice and humans and protects motoneurons against ischemic death. Nat Genet 2003;34:383–394.
37. Gros-Louis F, Laurent S, Lopes AA, et al. Absence of mutations in the hypoxia response element of VEGF in ALS. Muscle Nerve 2003;28:774–775.
38. Kawahara Y, Ito K, Sun H, et al. Low editing efficiency of GluR2 mRNA is associated with a low relative abundance of ADAR2 mRNA in white matter of normal human brain. Eur J Neurosci 2003;18:23–33.
39. Venter JC, Adams MD, Myers EW, et al. The sequence of the human genome. Science 2001;291:1304–1351.
40. Colbert MC, Rubin WW, Linney E, LaMantia AS. Retinoid signaling and the generation of cellular diversity in the embryonic mouse spinal cord. Dev Dyn 1995;204:1–12.
41. Sakakibara S, Okano H. Expression of neural RNA-binding proteins in the postnatal CNS: implications of their roles in neuronal and glial cell development. J Neurosci 1997;17: 8300–8312.
42. Puls I, Jonnakuty C, LaMonte BH, et al. Mutant dynactin in motor neuron disease. Nat Genet 2003;33:455–456.
43. Williamson TL, Cleveland DW. Slowing of axonal transport is a very early event in the toxicity of ALS-linked SOD1 mutants to motor neurons. Nat Neurosci 1999;2:50–56.
44. Zhang B, Tu P, Abtahian F, et al. Neurofilaments and orthograde transport are reduced in ventral root axons of transgenic mice that express human SOD1 with a G93A mutation. J Cell Biol 1997;139:1307–1315.
45. Farah CA, Nguyen MD, Julien JP, Leclerc N. Altered levels and distribution of microtuble-associated protein before disease onset in a mouse model of amyotrophic lateral sclerosis. J Neurochem 2003;84:77–86.

46. Ideguchi H, Ueda A, Tanaka M, et al. Structural and functional characterization of the USP11 deubiquitinating enzyme, which interacts with the RanGTP-associated protein RanBPM. Biochem J 2002;367:87–95.
47. Hensley K, Floyd RA, Gordon B, et al. Temporal patterns of cytokines and apoptosis-related gene expression in spinal cords of the G93A-SOD1 mouse model of amyotrophic lateral sclerosis. J Neurochem 2002;82:365–374.
48. Hall ED, Oostveen JA, Gurney ME. Relationship of microglial and astrocytic activation to disease onset and progression in a transgenic model of familial ALS. Glia 1998;23:249–256.
49. Mu X, He J, Anderson DW, et al. Altered expression of bcl-2 and bax mRNA in amyotrophic lateral sclerosis spinal cord motor neurons. Ann Neurol 1996;40:379–386.
50. Ekegren T, Grundstrom E, Lindholm D, Aquilonius SM. Up-regulation of Bax protein and increased DNA degradation in ALS spinal cord motor neurons. Acta Neurol Scand 1999;100: 317–321.
51. Ranganathan S, Bowser R. Alterations in G(1) to S phase cell-cycle regulators during amyotrophic lateral sclerosis. Am J Pathol 2003;162:823–835.
52. Malaspina A, de Belleroche J. Spinal cord molecular profiling provides a better understanding of amyotrophic lateral sclerosis pathogenesis. Brain Res Brain Res Rev 2004;45:213–229.
53. Sobue G, Sahashi K, Takahashi A, et al. Degenerating compartment and functioning compartment of motor neurons in ALS: possible process of motor neuron loss. Neurology 1983;33: 654–657.

doi:10.1093/brain/awh381 *Brain* (2005), **128**, 659–670

Widespread nuclear and cytoplasmic accumulation of mutant androgen receptor in SBMA patients

Hiroaki Adachi,[1] Masahisa Katsuno,[1] Makoto Minamiyama,[1] Masahiro Waza,[1] Chen Sang,[1] Yuji Nakagomi,[2] Yasushi Kobayashi,[1] Fumiaki Tanaka,[1] Manabu Doyu,[1] Akira Inukai,[1] Mari Yoshida,[3] Yoshio Hashizume[3] and Gen Sobue[1]

[1]*Department of Neurology, Nagoya University Graduate School of Medicine, Nagoya,* [2]*Central Research Laboratories, School of Medicine, Aichi Medical University and* [3]*Department of Neuropathology, Institute for Medical Sciences of Aging, Aichi Medical University of Aichi, Japan*

Correspondence to: Gen Sobue, MD, PhD, Department of Neurology, Nagoya University Graduate School of Medicine, 65 Tsurumai-cho Showa-ku, Nagoya, 466-8550, Japan
E-mail: sobueg@med.nagoya-u.ac.jp

Summary

Spinal and bulbar muscular atrophy (SBMA) is an inherited adult onset motor neuron disease caused by the expansion of a polyglutamine (polyQ) tract within the androgen receptor (AR), affecting only males. The characteristic pathological finding is nuclear inclusions (NIs) consisting of mutant AR with an expanded polyQ in residual motor neurons, and in certain visceral organs. We immunohistochemically examined 11 SBMA patients at autopsy with 1C2, an antibody that specifically recognizes expanded polyQ. Our study demonstrated that diffuse nuclear accumulation of mutant AR was far more frequent and extensive than NIs being distributed in a wide array of CNS nuclei, and in more visceral organs than thus far believed. Mutant AR accumulation was also present in the cytoplasm, particularly in the Golgi apparatus; nuclear or cytoplasmic predominance of accumulation was tissue specific. Furthermore, the extent of diffuse nuclear accumulation of mutant AR in motor and sensory neurons of the spinal cord was closely related to CAG repeat length. Thus, diffuse nuclear accumulation of mutant AR apparently is a cardinal pathogenetic process underlying neurological manifestations, as in SBMA transgenic mice, while cytoplasmic accumulation may also contribute to SBMA pathophysiology.

Keywords: polyglutamine; spinal and bulbar muscular atrophy; diffuse nuclear accumulation; nuclear inclusion, cytoplasmic accumulation

Abbreviations: polyQ = polyglutamine; SBMA = spinal and bulbar muscular atrophy; AR = androgen receptor; NIs = nuclear inclusions; DRPLA = dentatorubral-pallidoluysian atrophy; CBP = CREB-binding protein

Received June 15, 2004. First revision August 23, 2004. Second revision November 26, 2004. Accepted November 30, 2004. Advance Access publication January 19, 2005

Introduction

Polyglutamine (polyQ) diseases are inherited neurodegenerative disorders caused by expansion of a trinucleotide CAG repeat in the causative genes. To date, nine polyQ diseases have been identified (Ross, 2002). Spinal and bulbar muscular atrophy (SBMA) is a polyQ disease involving mainly spinal and brainstem motor neurons (Kennedy *et al.*, 1968; Sobue *et al.*, 1989). In SBMA, a polymorphic CAG repeat ordinarily consisting of 14–32 CAGs is expanded to 40–62 CAGs in the first exon of the androgen receptor (AR) gene (La Spada *et al.*, 1991; Tanaka *et al.*, 1996), and shows somatic mosaicism (Tanaka *et al.*, 1999). An inverse correlation exists between CAG repeat size and age at onset as well as disease severity in SBMA (Doyu *et al.*, 1992; Igarashi *et al.*, 1992; La Spada *et al.*, 1992). SBMA patients develop premature muscular exhaustion, and subsequently slowly progressive muscular weakness, atrophy and fasciculations in bulbar and limb muscles (Kennedy *et al.*, 1968; Sobue *et al.*, 1989; Sperfeld *et al.*, 2002). SBMA patients may also have mild sensory impairment, which usually remains subclinical (Sobue *et al.*, 1989; Li *et al.*, 1995; Mariotti *et al.*, 2000). Besides these symptoms of neuronal degeneration, androgen insensitivity symptoms such as gynaecomastia, testicular atrophy and reduced fertility are common (Arbizu *et al.*, 1983). Elevated serum creatine kinase concentrations, impaired glucose tolerance, hepatic dysfunction and hyperlipidaemia are frequent (Sobue *et al.*, 1989; Li *et al.*, 1995). These findings show that involvement of

SBMA is not restricted to motor neurons, but extends to several visceral organs.

The cardinal pathological findings of SBMA are motor neuron loss in the spinal cord and brainstem (Sobue *et al.*, 1989) and the presence of the nuclear inclusions (NIs), representing mutant AR, in residual motor neurons in brainstem motor nuclei, in spinal motor neurons (Li *et al.*, 1998*a*) and in certain visceral organs (Li *et al.*, 1998*b*). However, diffuse nuclear accumulation of the mutant protein has been detected in a more widespread distribution than NIs in a transgenic mouse model of SBMA (Katsuno *et al.*, 2002, 2003; Adachi *et al.*, 2003) and in models of other polyQ diseases (Schilling *et al.*, 1999; Yvert *et al.*, 2000; Lin *et al.*, 2001). Such accumulation has been found to be relevant to neuronal dysfunction and eventual symptom appearance. Indeed, in dentatorubral-pallidoluysian atrophy (DRPLA), tissue distribution of diffuse nuclear accumulation of the responsible mutant protein was more widespread and more relevant to the disease severity and symptoms than that of NIs (Yamada *et al.*, 2001*a*, *b*).

Recently we demonstrated in our transgenic mouse model that diffuse nuclear mutant AR accumulation can be prevented by reduction of circulating testosterone with castration or with an anti-androgenic agent such as leuprolerin; in treated animals, motor function and survival rate were dramatically improved (Katsuno *et al.*, 2002, 2003), suggesting that disease manifestation in SBMA is highly testosterone dependent (Lieberman *et al.*, 2002; Walcott and Merry, 2002*a*; Chevalier-Larsen *et al.*, 2004). Indeed, a female carrier of SBMA, even if homozygous, does not express disease phenotypes (Sobue *et al.*, 1993; Schmidt *et al.*, 2002), presumably because circulating testosterone concentrations are low. These observations indicate that nuclear translocation and nuclear accumulation of mutant AR, detected as diffuse nuclear accumulation, is closely linked to the phenotypic expressions and that diffuse nuclear mutant AR accumulation is of major pathogenetic importance in neuronal dysfunction (Katsuno *et al.*, 2002, 2003).

In this study, to understand better the pathophysiology of SBMA, we examined neural and non-neural tissue distributions of mutant AR accumulation in 11 SBMA patients at autopsy, using 1C2, an antibody specific for the expanded polyQ tract, as well as antibodies against AR. First, diffuse nuclear accumulation of mutant AR was far more extensive than that of NIs. Secondly, mutant AR accumulation was also present in cytoplasm, specifically in the Golgi apparatus, with predominance of nuclear or cytoplasmic accumulation being tissue specific. Thirdly, the extent of diffuse nuclear accumulation was closely related to CAG repeat length. Our present results strongly suggested that diffuse nuclear accumulation of mutant AR is of critical pathogenetic importance for motor symptoms as in the SBMA transgenic mouse model, although cytoplasmic accumulation may also contribute to the pathophysiology of SBMA.

Subjects and methods

Patients

Eleven patients with clinicopathologically and genetically confirmed SBMA (age at death, 51–84 years; mean, 66) were examined in this study (Table 1). These patients had been hospitalized and followed-up at Nagoya University Hospital and its affiliated hospitals during the past 25 years. Age at onset ranged between 20 and 75 years, and muscle weakness and bulbar symptoms had progressed for 6–53 years. Elevated serum creatine kinase and glucose was observed in many patients. Causes of death included respiratory failure related to pneumonia in seven patients, lung cancer and colon cancer in one patient each, and tuberculosis and suffocation in one patient each. At autopsy, the brain, spinal cord, dorsal root ganglia, thoracic sympathetic ganglia and various visceral organs were removed and fixed in 10% buffered formalin solution. CAG repeat length in the *AR* gene ranged between 40 and 50. Five other subjects (age 60–74 years, mean 67.3) who died of non-neurological diseases served as controls.

Tissue preparation and immunohistochemistry

We prepared 5 μm thick, formalin-fixed, paraffin-embedded sections of various portions of the cerebrum, brainstem, cerebellum,

Table 1 *Clinical features of 11 SBMA patients*

Patient	Age at death (years)	Onset of limb weakness (years)	CK (normal range)	Glucose (mg/dl)	$(CAG)_n$	Cause of death
1	74	20	455 (57–197)	84*	48	Pneumonia
2	60	27	477 (36–203)	276	50	Pneumonia
3	71	50	995 (53–288)	141	48	Pneumonia
4	60	40	191 (32–197)	134	44	Lung cancer
5	78	25	411 (30–170)	362	42	Pneumonia
6	84	75	75 (<110)	100	40	Tuberculosis, silicosis
7	51	41	712 (30–170)	96*	47	Pneumonia
8	66	41	471 (<120)	163	48	Pneumonia
9	72	39	45 (<25)	101*	43	Colon cancer
10	59	53	301 (8–80)	105*	ND	Suffocation
11	51	27	173 (20–100)	101	ND	Pneumonia

CK = serum creatine kinase; $(CAG)_n$ = number of expanded CAG repeats in the AR allele. $(CAG)_n$ was determined on the DNA from blood samples (patients 1–7) or from stored tissue samples (patients 8 and 9, liver). *Impaired glucose tolerance assessed with 75 g oral glucose tolerance test. ND = not determined.

spinal cord, dorsal root ganglia, sympathetic ganglia, pituitary gland, peripheral nerve, muscle and non-neural visceral organs from SBMA and control subjects. Sections then were deparaffinized and rehydrated through a graded series of alcohol–water solutions. For the mutant AR immunohistochemical study, sections were pre-treated with immersion in 98% formic acid for 5 min and then with microwave oven heating for 10 min in 10 mM citrate buffer at pH 6.0. Sections were blocked with normal serum from the animal species in which each second antibody was raised (1 : 20), and then incubated with a mouse anti-expanded polyQ antibody (Trottier *et al.*, 1995) (1C2; Chemicon, Temecula, CA; 1 : 10 000); a mouse anti-Golgi 58K protein antibody (Sigma, St. Louis, MO; 1 : 100); rabbit polyclonal antibody N-20 (Santa Cruz Biotechnology, Santa Cruz, CA; 1 : 200); rabbit polyclonal antibody PG-21 (Affinity BioReagents, Golden, CO; 1 : 200); rabbit polyclonal antibody H-280 (Santa Cruz; 1 : 200); rabbit polyclonal antibody C-19 (Santa Cruz; 1 : 200); or a mouse monoclonal antibody (Ab-1; Neomarkers, Fremont, CA; ready-to-use) against human AR protein. Then the sections were incubated with biotinylated IgG raised against the species used for each primary antibody (Vector Laboratories, Burlingame, CA). Immune complexes were visualized using streptavidin–horseradish peroxidase (Dako, Glostrup, Denmark) and 3,3′-diaminobenzidine (Dojindo, Kumamoto, Japan) substrate. Sections were counterstained with methyl green or Mayer's haematoxylin. As a negative control, primary antibodies were replaced with normal rabbit or mouse serum. The population of labelled neurons was analysed semi-quantitatively in all 11 SBMA patients, and non-neural visceral organs in nine patients (patients 1–8, and 11) by counting the positive and negative cells for labelling in the region of interest and graded as – to +++.

To assess the co-localization of cytoplasmic mutant AR accumulation and cell organelles, five selected SBMA patients (patients 1, 2, 6, 8 and 10) were analysed by double immunofluorescence staining. The sections were blocked with 5% normal serum and then sequentially incubated at 4°C overnight with any antibody to lysosomal markers, anti-cathepsin B antibody (Ab-3; Oncogene, Cambridge, MA; 1 : 20), anti-cathepsin D antibody (Ab-2; Oncogene; 1 : 20), anti-cathepsin K antibody (N-20; Santa Cruz Biotechnology; 1 : 50), anti-cathepsin L antibody (S-20; Santa Cruz Biotechnology; 1 : 50), antibody to Golgi apparatus, anti-human TGN46 antibody (Serotec, Oxford, UK; 1 : 1000), antibody to endoplasmic reticulum marker, anti-GRP78 antibody (N-20; Santa Cruz; 1 : 200), or antibody to mitochondria, anti-mitochondria antibody (Chemicon; 1 : 50), and 1C2 antibody (Chemicon; 1 : 10 000). Sections were incubated with Alexa 488-conjugated anti-mouse IgG (Molecular Probes, Leiden, The Netherlands; 1 : 1300) and Alexa 568-conjugated IgG raised against the species used for each primary antibody (Molecular Probes; 1 : 1000). For double immunofluorescence staining using anti-human TGN46 antibody, sections were incubated with biotinylated anti-sheep IgG (Vector Laboratories; 1 : 400) for 8 h at 4°C, the sections were incubated with Alexa 568-conjugated streptavidin (Molecular Probes; 1 : 1000) and Alexa 488-conjugated anti-mouse IgG (Molecular Probes; 1 : 1300) for 2 h at 4°C. Sections then were examined and photographed using a confocal laser scanning microscope (MRC 1024; Bio-Rad Laboratories, Hercules, CA).

For electron microscopic immunohistochemistry, buffered formalin-fixed, paraffin-embedded tissue sections were deparaffinized, rehydrated, immunostained with 1C2 antibody (Chemicon, 1 : 10 000), and then incubated with biotinylated anti-mouse IgG (Vector Laboratories; 1 : 1300). Immunoreactivity in tissue sections was visualized using streptavidin–horseradish peroxidase (Dako) and 3,3′-diaminobenzidine substrate (Dojindo), fixed with 2% osmium tetroxide in 0.1 mol/l phosphate buffer at pH 7.4, dehydrated in graded alcohol–water solutions, and embedded in epoxy resin. Ultrathin sections then were cut for observation under an electron microscope (H-7100; Hitachi High-Technologies Corporation, Tokyo, Japan).

Quantification of diffuse nuclear- and NI-positive cell populations

For quantitative assessment, we prepared at least 100 transverse sections each from the cervical, thoracic and lumbar spinal cord for staining with 1C2 antibody as above. The numbers of 1C2-positive and -negative cells in the ventral and dorsal horn on both right and left sides were counted on every 10th section under the light microscope with a computer-assisted image analyser (Luzex FS; Nikon, Tokyo, Japan). For the purposes of counting, a cell was defined by the presence of its nucleus in a given 5 μm thick section. Diffuse nuclear staining and NI-positive neurons were assessed separately. Neurons showing both diffuse nuclear staining and NIs were counted in both categories. The area of the ventral and dorsal horn of each spinal cord section was determined as described previously (Terao *et al.*, 1996; Adachi *et al.*, 2001). Populations of 1C2-positive cells were expressed as percentages of the total neuronal count. For statistical analysis, mean values of these percentages in sections examined from each of the cervical, thoracic and lumbar spinal segments for each patient were obtained.

Statistical analysis

We analysed the data by Pearson's correlation coefficient and Spearman's rank correlation as appropriate using Statview software (version 5; Hulinks, Tokyo, Japan), considering P values <0.05 to be indicative of significance.

Results

Immunohistochemical localization of mutant androgen receptor in the neural tissues

In all 11 patients with SBMA, NIs were visualized clearly with 1C2 (Fig. 1). In addition to NIs, diffusely distributed staining with 1C2 was observed in neuronal nuclei (Fig. 1). Among nuclei with diffuse staining, some showed punctate, granular or web-like patterns, while others showed intense diffuse staining (Fig. 1). In some neurons, NIs and diffuse nuclear staining co-existed (Fig. 1). Moreover, occasional neurons showed granular or punctate 1C2-positive accumulation in the cytoplasm (Fig. 1). As reported previously (Li *et al.*, 1998*a*, *b*), NIs were observed frequently in lower motor neurons, which are known to be affected in this disease. However, we found that neuronal nuclear and cytoplasmic accumulations extended to various regions of the nervous system previously reported to be spared (Li *et al.*, 1998*a*, *b*), including the striatum, caudate nucleus, mammillary body, thalamus, hypothalamus, reticular formation, red nucleus, substantia nigra, locus coerulus, nucleus raphe pontis, pontine nuclei, cuneate nucleus, nucleus ambiguus, gracile nucleus, supraspinal nucleus, cerebellar dentate nucleus, Clarke's

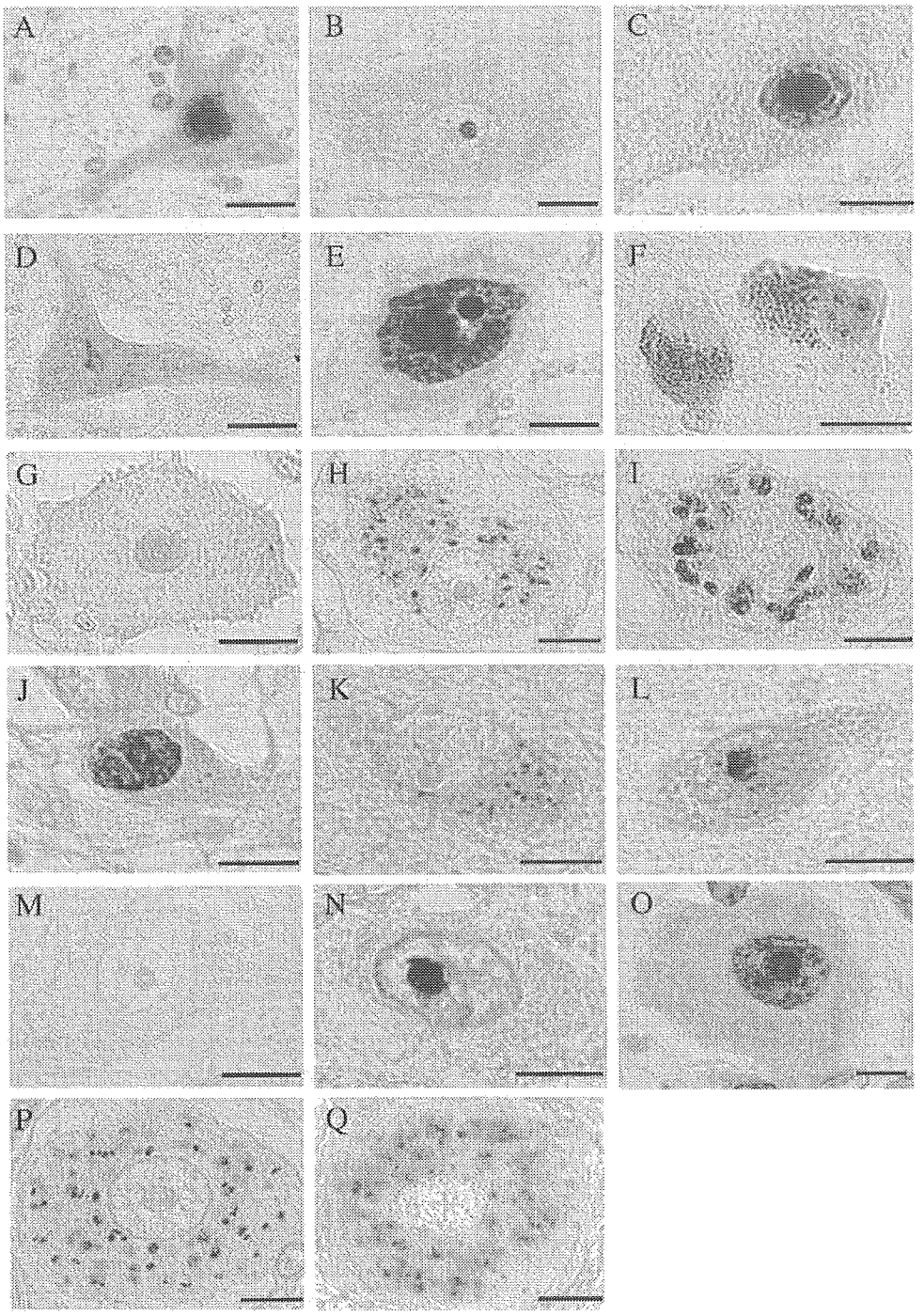

Fig. 1 Immunohistochemical analysis in the neural tissues from SBMA patients and control cases. In the CNS of SBMA patients, intense diffuse nuclear staining is present in neuronal nuclei of various regions using 1C2 antibody (**A**, **E**, **F**, **G**, **J** and **L**). Diffuse immunostaining of mutant androgen receptor (AR) is present in a web-like pattern in nuclei of anterior horn neurons (**A**). Diffuse nuclear staining is also observed in posterior horn neurons (**E**), substantia nigra (**F**), spinal dorsal root ganglia (**G**), paravertebral sympathetic ganglia (**J**) and hypothalamus (**L**). Some nuclei appear packed with mutant AR. Small or large nuclear inclusions are also stained intensely using 1C2 antibody in anterior horn neurons (**B–D**), posterior horn neurons (**E**), the substantia nigra (**F**) and the hypothalamus (**L**). Most of the dark brown pigment seen in the neuronal cytoplasm in the substantia nigra (**F**) is neuromelanin. In addition to nuclear inclusions, occasional neurons exhibit granular structures immunoreactive for 1C2 in the cytoplasm, such as in the anterior horn (**D**) and hypothalamus (**K**). In spinal dorsal root ganglia, small or large cytoplasmic inclusions are frequent (**H** and **I**). There is no immunoreactivity for 1C2 in the spinal anterior horn cell from the control case (**M**). Immunopositive nuclear inclusions and diffuse nuclear staining are also present using H280 antibody in the spinal anterior horn cell (**N**) and spinal dorsal root ganglia (**O**). Spinal dorsal root ganglia neurons exhibit granular structures immunoreactive for anti-Golgi 58K protein antibody in the cytoplasm in SBMA (**P**) and a control case (**Q**). Scale bars = 20 μm for **A**, **D**, **F**, **G**, **M** and **O**; and 10 μm for **B**, **C**, **E**, **H**, **I**, **J**, **K**, **L**, **N**, **P** and **Q**.

nucleus, posterior horn and intermediolateral nucleus of the spinal cord, dorsal root ganglia and sympathetic ganglia (Fig. 1, Table 2). Cytoplasmic inclusions were prominent in the dorsal root ganglia neurons, and some neurons in the mammillary body, hypothalamus and facial motor nucleus and anterior and posterior horns of the spinal cord showed a slight degree of cytoplasmic accumulation (Table 2). We detected both nuclear and cytoplasmic accumulations in some neurons (Fig. 1D). No significant difference in staining pattern was evident between regions previously reported to be affected and unaffected. Diffuse nuclear staining was seen more frequently than NIs in most regions (Table 2). Relative numbers of stained neurons varied between patients, but no staining was detected in cerebral cortex, hippocampus or cerebellar cortex. In contrast to neurons, NIs and diffuse nuclear staining were very rare in glial cells. NIs stained strongly with anti-ubiquitin antibody, while cytoplasmic accumulations did not (data not shown). Anti-human AR antibodies also recognized NIs (Fig. 1N), and occasionally stained diffuse nuclear accumulations (Fig. 1O). However, cytoplasmic accumulations were not seen with anti-AR antibodies.

Table 2 *Immunohistochemical distribution of mutant AR in the neural tissues of patients with SBMA*

Region	Nuclear accumulation		Cytoplasmic accumulation
	Diffuse nuclear accumulation	NI	
Cerebrum			
Cerebral cortex	−	−	−
Striatum	+	+	−
Caudate nucleus	+	+	−
Mammillary body	−	−	+
Thalamic nuclei	+	+	−
Hypothalamus	+ to ++	+	+
Midbrain			
Superior colliculus	−	−	−
Periaqueductal grey	+	+	−
Oculomotor nucleus	−	−	−
Reticular formation of midbrain	+	+	−
Red nucleus	+	+	−
Substantia nigra	+	+	−
Pons			
Locus coerulus	+	+	−
Trigeminal motor nucleus	+ to ++	+	−
Reticular formation of pons	+	+	−
Facial motor nucleus	+ to +++	+	+
Nucleus raphe pontis	+	+	−
Pontine nuclei	+	+	−
Medulla			
Cuneate nucleus	+	+	−
Hypoglossal nucleus	+ to ++	+	−
Nucleus ambiguus	+ to ++	+	−
Gracile nucleus	+	+	−
Supraspinal nucleus	+ to ++	+	−
Accessory nucleus	+	+	−
Cerebellum			
Purkinje cell	−	−	−
Granule cell	−	−	−
Cerebellar dentate nucleus	+	+	−
Spinal cord			
Anterior horn motor neurons	+ to +++	+ to ++	+
Intermediate zone	+	+	−
Clarke's nucleus	+	−	−
Posterior horn neurons	+ to ++	− to +	+
Intermediolateral nucleus	+	+	
Dorsal root ganglia	+	+	++ to +++
Sympathetic ganglia	+	+	−

Frequency of neurons expressing polyglutamine immunoreactivity: −, 0%; +, 0–4%; ++, 4–8%; +++, 8%.

Electron microscopic immunohistochemistry for 1C2 demonstrated granular dense aggregates without a limiting membrane corresponding to NIs and cytoplasmic accumulations, whereas amorphous aggregates corresponded to diffuse nuclear staining in neurons (Fig. 2). No filamentous structures such as those reported in Huntington's disease, DRPLA and Machado–Joseph disease were seen. Neural tissues from five control cases were also examined in the same manner as that for SBMA cases; in these, NIs, diffuse nuclear staining and cytoplasmic accumulations were not seen, indicating that the immunohistochemical procedure with the highly diluted condition of 1C2 applied in this study did not recognize the TATA-binding protein, a transcription factor containing a stretch of polyQ residues (Trottier *et al.*, 1995), as previously demonstrated (Yamada *et al.*, 2001*a*, 2002*a*).

Although we did not quantitatively examine neuronal populations in this study, the motor neurons in the spinal cord and brainstem showed the most conspicuous depletion, as expected. Neurons in the posterior horn of the spinal cord, where diffuse nuclear accumulations and NIs were present in relatively high frequency, also appeared to be depleted to some extent. Quantitative assessment of neuronal cell populations in regions newly showing mutant AR accumulation will be needed.

Co-localization of cytoplasmic organelles with mutant AR

We performed immunofluorescence with double staining using primary antibodies to recognize specifically various cytoplasmic cell organelles together with 1C2 in the dorsal root ganglia, where cytoplasmic mutant AR accumulation was most prominent (Table 2). TGN46 and 1C2 were co-localized (Fig. 3), indicating that mutant AR exists in the Golgi apparatus. Spinal dorsal root ganglia neurons exhibit some granular structures immunoreactive for another Golgi apparatus marker anti-Golgi 58K protein antibody in the cytoplasm (Fig. 1P and Q). Other organelle markers, including antibodies for lysosomes, endoplasmic reticulum and mitochondria, did not show co-localization with 1C2 (Fig. 3), indicating that expanded polyQ sequences were not detected in these organelles.

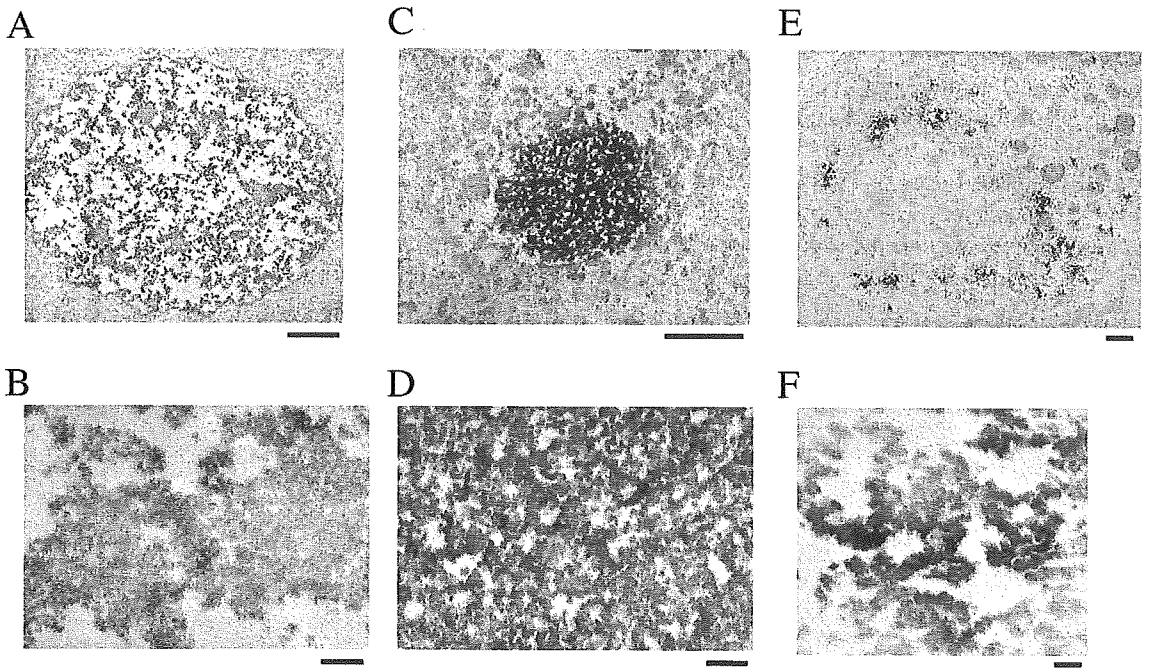

Fig. 2 Electron microscopic immunohistochemical study of nuclear inclusions in motor neurons, and of diffuse nuclear staining and cytoplasmic inclusions in sensory neurons. Electron microscopic immunohistochemistry using 1C2 demonstrated amorphous aggregates corresponding to diffuse nuclear staining in the spinal dorsal root ganglia (**A** and **B**), and granular dense aggregates without fibrous configurations corresponding to nuclear and cytoplasmic inclusions in the spinal anterior neuron (**C** and **D**) and spinal dorsal root ganglia (**E** and **F**). Scale bars = 2 μm for **A**, **C** and **E**; and 200 nm for **B**, **D** and **F**.

Correlation of diffuse nuclear accumulation and NIs with degree of CAG repeat expansion

We examined the correlation of diffuse nuclear accumulation and NIs with the degree of CAG repeat expansion in anterior and posterior horn spinal cord neurons. Averaged frequencies of diffuse nuclear accumulations and NIs in cervical, thoracic and lumbar spinal segments were evaluated for correlation with numbers of CAG repeats in the *AR* gene. The frequency of diffuse nuclear accumulation in anterior and posterior horn neurons correlated well with the degree of CAG repeat expansion (Fig. 4; $r = 0.78$, $P < 0.05$ and $r = 0.69$, $P < 0.05$, respectively). However, the frequency of NIs in motor neurons and posterior horn neurons did not show a significant correlation with number of CAG repeats (Fig. 4; $r = 0.05$, P = NS and $r = -0.14$, P = NS, respectively). These observations strongly suggest that diffuse nuclear accumulation of the mutant AR protein is more important pathogenetically than NIs.

Immunohistochemical localization of mutant AR in non-neural tissues

As in neural tissues, diffuse nuclear accumulations, NIs or cytoplasmic accumulations of mutant AR were observed in certain visceral organs and skin (Fig. 5, Table 3). Diffuse nuclear accumulations and NIs were detected in the liver, proximal tubules of the kidney, testis, prostate gland, and scrotal and other skin (Fig. 5, Table 3). Cytoplasmic accumulations were detected in the liver, pancreatic islets of Langerhans, testis and prostate gland (Fig. 5, Table 3). Nuclear labelling and cytoplasmic accumulation both were absent in the pituitary gland, heart, lung, intestine, spleen, thyroid, adrenal gland and skeletal muscles. Pancreatic islet cells showed exclusively cytoplasmic accumulations without detectable nuclear accumulations, suggesting that the impaired glucose tolerance frequently observed in our patients (Table 1) could be attributed to cytoplasmic mutant AR accumulation. Ubiquitin staining detected only NIs and, as observed in neural tissues, anti-human AR antibodies occasionally showed diffuse nuclear accumulation without cytoplasmic staining (Fig. 5J). The five control cases did not show any 1C2 immunoreactivity in viscera or skin.

Discussion

The present study clearly demonstrated that diffuse nuclear accumulation of mutant AR, detected by the antibody 1C2 which specifically recognizes the expanded polyQ tract, occurred more frequently than NIs in neural and non-neural tissues in SBMA patients. In neural tissues, diffuse nuclear mutant AR accumulation occurred in the basal ganglia, thalamus, hypothalamus, various midbrain, pontine and medullary nuclei, posterior horn, intermediolateral and Clarke's nuclei of the spinal cord and in sensory and sympathetic ganglion neurons, as well as brainstem and spinal cord motor neurons. NIs detected by 1C2 were similar

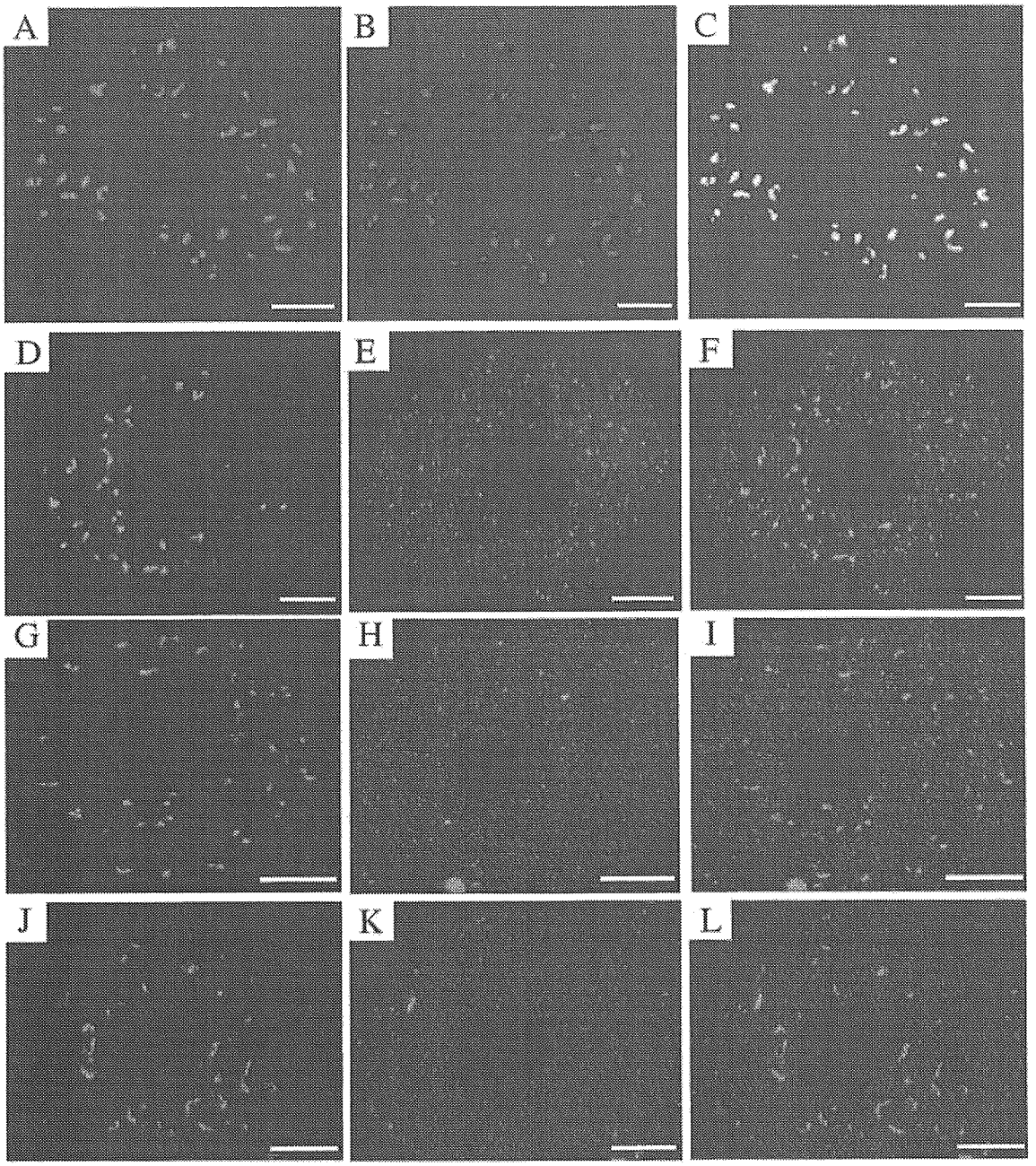

Fig. 3 Co-localization of organelles with mutant AR accumulation. Double immunofluorescence staining with antibodies against TGN46 and expanded polyQ reveals that TGN46 and mutant androgen receptor (AR) are co-localized, as shown for (**A**) expanded polyQ (green), (**B**) TGN46 (red) and (**C**) superimposition of the two signals (yellow) in neurons of the spinal dorsal root ganglia in SBMA, suggesting that mutant AR exists in the Golgi apparatus. Cytoplasmic co-localization of cathepsin B (**E**), GRP78 (**H**) and mitochondria (**K**) with mutant AR (**D**, **G** and **J**) is not observed in dorsal root ganglia (shown in **F**, **I** and **L**), suggesting that the endoplasmic reticulum, lysosomes and mitochondria are unassociated with mutant AR. Scale bars = 10 μm for **A**–**L**.

in distribution to diffuse nuclear accumulation, but the frequency of NIs in each tissue was far less than for diffuse nuclear accumulation. We previously demonstrated that diffuse nuclear mutant AR protein accumulation was more extensive than NIs in male SBMA transgenic mice (Katsuno *et al.*, 2002, 2003). Furthermore, expression and severity of motor dysfunction, and abatement of abnormalities when the mice were castrated or given leuprolerin, paralleled the extent of diffuse nuclear mutant AR accumulation rather than that of NIs (Katsuno *et al.*, 2002, 2003). Accordingly, neuronal dysfunction appeared to be closely related to diffuse nuclear mutant AR accumulation. The key observation in the present study was a significant close correlation between frequency of diffuse nuclear mutant AR accumulation and length of CAG repeat expansion, while a similar correlation was not observed between frequency of NIs and CAG repeats. Diffuse nuclear

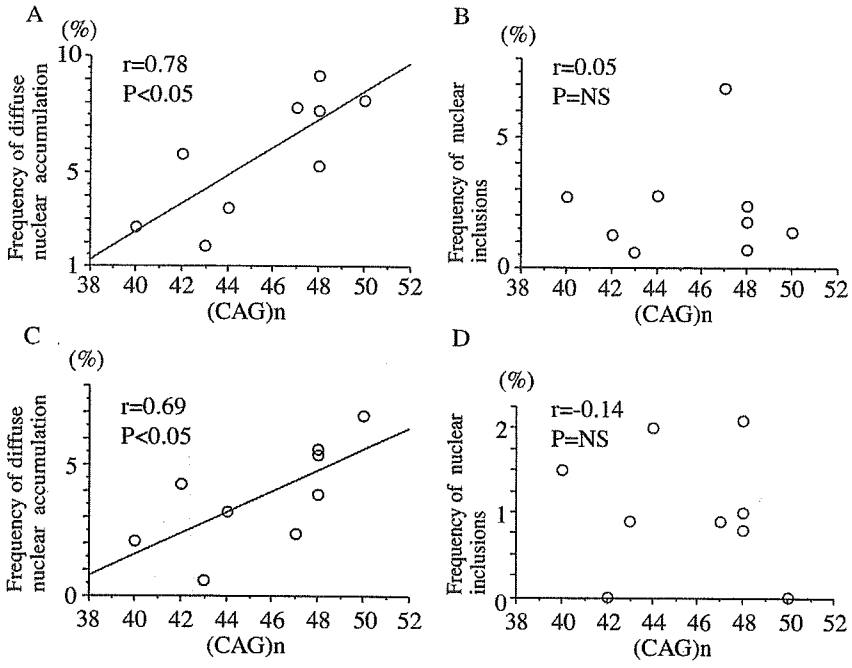

Fig. 4 The relationship of the number of CAG repeats to the frequency of diffuse nuclear accumulation and nuclear inclusions. Diffuse nuclear staining correlates significantly with the number of CAG repeats in anterior horn neurons (**A**) and posterior horn neurons (**C**). On the other hand, nuclear inclusions do not correlate significantly with the number of CAG repeats in the anterior horn neurons (**B**) or posterior horn neurons (**D**).

mutant protein accumulation also has been demonstrated in the neural tissues affected by DRPLA (Yamada *et al.*, 2001*a*, 2002*a*), Huntington's disease (Sapp *et al.*, 1997) and Machado–Joseph disease (Yamada *et al.*, 2001*b*) as well as corresponding transgenic mouse models (Schilling *et al.*, 1999; Yvert *et al.*, 2000; Lin *et al.*, 2001); and, here too, diffuse nuclear mutant protein accumulation was more widespread and extensive than NIs in DRPLA patients. These observations are in good agreement with our present observation in SBMA patients; together, they suggest that diffuse nuclear accumulation of mutant proteins with an expanded polyQ tract is an early event prior to NI formation that is closely related to manifestation of neuronal dysfunction (Yamada *et al.*, 2001*a*; Garden *et al.*, 2002; Katsuno *et al.*, 2002, 2003; Watase *et al.*, 2002; Yoo *et al.*, 2003). However, the molecular pathogenetic process by which diffuse nuclear mutant AR accumulation induces neuronal dysfunction still is unclear. Although considerable controversy recently surrounds the importance of NIs in the pathophysiology in polyQ diseases (Simeoni *et al.*, 2000; Walcott and Merry, 2002*b*; Bates, 2003; Michalik and Van Broeckhoven, 2003; Ross *et al.*, 2003), our data showed that diffuse mutant AR accumulation in nuclei could have potent cytotoxic effects inducing neuronal dysfunction through an active epitope of the expanded polyQ tract.

Anti-AR antibodies showed the ability to detect NIs, and some of them (H280, N-20 and Ab-1) occasionally stained diffuse nuclear accumulations. Diffuse nuclear accumulation had the appearance of amorphous aggregates of mutant AR as observed by electron microscopic immunohistochemistry using 1C2 (Fig. 2) (Katsuno *et al.*, 2002). These observations suggest that the polyQ tract epitope can be detected by 1C2, while other AR protein epitopes may be protected by structural features of the aggregate state of the mutant AR. This view is supported by observations made by small-angle X-ray scattering and infrared spectroscopy carried out with myoglobin protein containing an inserted highly expanded polyQ tract, localizing the polyQ tract to the surface of aggregates, while other epitopes were sequestered within aggregates (Tanaka *et al.*, 2001, 2003). These observations suggest that 1C2 can detect the amorphous aggregate state of mutant AR protein, making 1C2 a more sensitive histological and pathophysiological marker than anti-AR protein antibodies. On the other hand, cytoplasmic accumulations were not seen with anti-AR antibodies. This cytoplasmic mutant AR was not ubiquitinated, in contrast to nuclear accumulated mutant AR, particularly the heavily ubiquitinated NIs, suggesting that protein modification varies between the nucleus and cytoplasm. Different protein modification might mask other AR protein epitopes directly or through structural alterations of the aggregate state of the mutant AR in the cytoplasm.

Another important observation in our study was the occurrence of cytoplasmic mutant AR accumulation in neural and non-neural tissues. In neural tissues, cytoplasmic accumulation was restricted to certain neuronal populations such as dorsal root ganglia neurons, mammillary body, hypothalamus, facial motor nucleus, and anterior and posterior horn neurons. In non-neural tissues, cytoplasmic accumulation also occurred in certain organs. Cytoplasmic mutant AR accumulation co-localized with a Golgi apparatus marker.

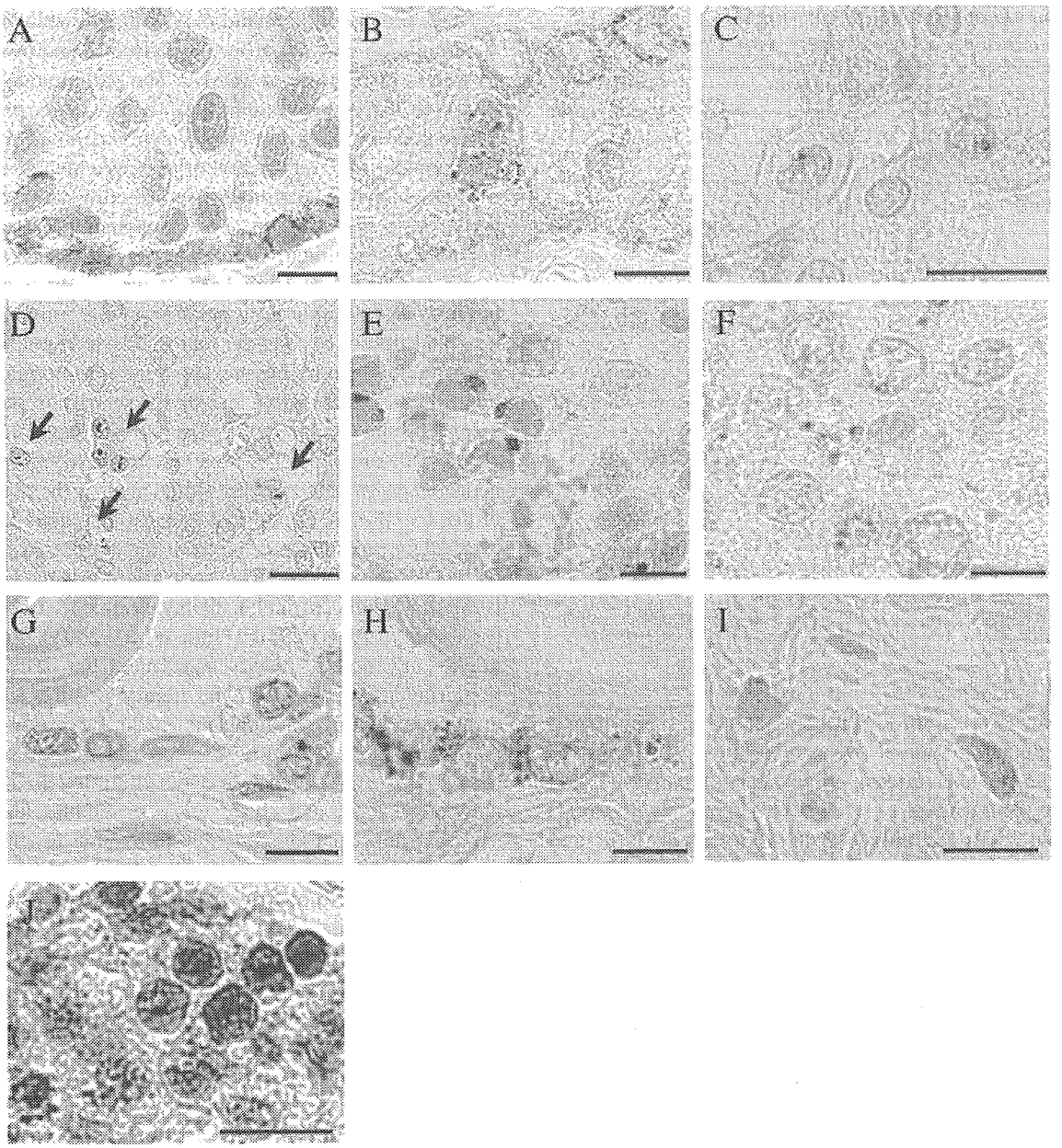

Fig. 5. Immunohistochemical study of the non-neural tissues in SBMA patients using 1C2 antibody. In the non-neural tissues, diffuse nuclear staining and nuclear inclusions are detectable in scrotal skin (**A**), other skin (**B**), proximal tubules of the kidney (**C**), hepatocytes (**D**), Sertoli cells of the testis (**E**), and glandular epithelium (**G**) and fibroblasts of the interstitial connective tissue (**I**) of the prostate gland. Moreover, cytoplasmic inclusions can be detected in hepatocytes (**D**), spermatocytes in the testis (**E**), pancreatic islets of Langerhans (**F**) and glandular epithelium of the prostate gland (**H**). Diffuse nuclear staining is also present using H280 antibody in Sertoli cells of the testis (**J**). Scale bars = 10 μm for **A**–**C** and **E**–**I**; and 20 μm for **D** and **J**.

Co-localization of a polyQ-expanded mutant protein with the Golgi apparatus has also been reported for ataxin-2 (Huynh *et al.*, 2003), although the significance of this localization remains unclear. Expression of polyQ-expanded mutant ataxin-2 disrupted the normal morphology of the Golgi complex and increased cell death (Huynh *et al.*, 2003). On the other hand, the lysosomal occurrence of other mutant proteins with an expanded polyQ tract has been reported in DRPLA (Yamada *et al.*, 2002*b*) and Huntington's disease (Sapp *et al.*, 1997). The lysosomal localization of polyQ-expanded mutant proteins suggests a lysosomal autophagic degradation process acting independently of the ubiquitin–proteasome pathway in the polyQ diseases (Sapp *et al.*, 1997). Additionally, the reason why neural tissues develop more nuclear than cytoplasmic accumulation while most involved visceral organs show equal or predominantly cytoplasmic accumulation is unknown. Differences in the predominant degradation pathway dealing with the mutant AR could influence the intracellular site of accumulation and eventual cell toxicity. One important question is whether cytoplasmic mutant AR

Table 3 *Immunohistochemical distribution of mutant AR in the non-neural tissues of patients with SBMA*

Region	Nuclear accumulation		Cytoplasmic accumulation
	Diffuse nuclear accumulation	NI	
Pituitary gland	–	–	–
Heart	–	–	–
Lung	–	–	–
Liver	+	+	+
Kidney	+ to ++	+	–
Pancreas	–	–	+ to ++
Intestine	–	–	–
Spleen	–	–	–
Thyroid	–	–	–
Adrenal gland	–	–	–
Testis	+ to ++	+	+ to ++
Prostate gland	+ to +++	+ to ++	+ to +++
Skeletal muscle	–	–	–
Scrotal skin	+ to +++	+	–
Skin	+ to ++	+	–

Frequency of cells expressing polyglutamine immunoreactivity: –, 0%; +, 0–3%; ++, 3–6%; +++, 6%.

accumulation exerts cytotoxicity in neural and non-neural tissues. Cytoplasmic mutant AR accumulation (Taylor *et al.*, 2003) as well as other mutant protein accumulations (Kegel *et al.*, 2000; Ravikumar *et al.*, 2002; Huynh *et al.*, 2003) involving an expanded polyQ tract in Golgi apparatus and lysosomes indeed has been found to induce cytotoxicity. Accumulation of mutant protein with expanded polyQ in the Golgi apparatus or lysosomes increases death of cultured cells through activation of apoptosis-related effectors such as caspase-3 (Ishisaka *et al.*, 1998; Kegel *et al.*, 2000; Huynh *et al.*, 2003). One should note that histologically or immunohistochemically evident mutant protein accumulation is not necessarily cytotoxic, while microaggregates at the molecular level that are histologically undetectable can also exert cytotoxicity. Indeed, excessive accumulation of mutant AR in aggresomes was found to protect cells from a cytotoxic form of mutant AR (Taylor *et al.*, 2003). However, our present study strongly suggests that these cytoplasmic mutant AR accumulations may be related to mutant AR-mediated cytotoxicity and eventual symptom manifestation. For instance, the pancreas showed only cytoplasmic mutant AR accumulation without obvious nuclear accumulation. Elevated serum glucose and impaired glucose tolerance were present in most of our patients, suggesting islet cell dysfunction in the pancreas. The frequency of cytoplasmic accumulations of mutant AR in pancreatic islet cells did not show a significant correlation with fasting blood glucose levels in the examined SBMA patients (data not shown), while certain symptoms and signs of SBMA apparently can be induced by cytoplasmic accumulation of mutant AR protein. Although further study of the significance of cytoplasmic mutant AR accumulation is needed, nuclear accumulation of the mutant AR protein appears to cause motor neuron dysfunction while cytoplasmic accumulation may underlie some visceral and possibly some neuronal dysfunction in SBMA. The pathological process is likely to differ between tissues, being more prominent in motor neuron nuclei, but mainly cytoplasmic in certain neuronal populations and visceral organs. We also need to clarify further which degradation process affecting mutant AR is most active in a given tissue, e.g. lysosomal in certain viscera versus via ubiquitination pathway in most neural tissues.

An important question here is why diffuse nuclear and possibly cytoplasmic accumulation of the mutant AR in the neuronal tissues beyond the major affected spinal and brainstem motor neurons has no apparent symptomatic involvement. First, the causative lesions for sensory impairment and essential-type tremor in SBMA patients have not yet been clearly substantiated. The novel lesion distribution of SBMA neurons shown in the present study, such as the posterior horn of the spinal cord, dorsal root ganglia, thalamus and cerebellum, might provide some explanations for these clinicopathological problems that have not been resolved. Since the cerebellothalamocortical pathway seems to be responsible for essential-type tremor (Pinto *et al.*, 2003), these lesions might contribute to mostly subclinical but definite sensory impairment and essential-type tremor in SBMA. Secondly, the occurrence of neuronal nuclear and cytoplasmic abnormalities in both clinically affected and non-affected neural regions in SBMA suggests that this alteration does not always induce neuronal cell dysfunction or death. The selective neuronal loss and dysfunction in neural lesions that are characteristic of SBMA might depend on additional factors that are specific to neurons in these systems. Recent studies have demonstrated that CREB-binding protein (CBP) is sequestered in AR-positive NIs, resulting in a decrease in CBP-dependent transcription (McCampbell *et al.*, 2000), and further histone acetylation is reduced in affected cells (McCampbell *et al.*, 2001; Steffan *et al.*, 2001; Minamiyama *et al.*, 2004). These reports suggest that CBP-dependent transcriptional dysregulations may cause symptomatic neuronal dysfunction. Since CBP-dependent transcriptional control differs among neurons, this difference may show the lack of their symptomatic involvement in certain polyQ-containing neurons. Alternatively, the population of neurons with nuclear accumulation of mutant AR in the regions beyond the commonly affected lesions may not be simply enough to manifest the responsible symptoms. A precise neuronal cell count assay combined with assessment of nuclear mutant AR accumulation will be needed to clarify these clinicopathological problems.

Clearly, motor neuron impairment with nuclear accumulation of mutant AR is the major problem in SBMA. Thus, for a therapeutic strategy against motor neuron dysfunction in SBMA, nuclear accumulation of mutant AR should be the main target, as we demonstrated in transgenic mice treated with leuprolerin. Cytoplasmic accumulation of mutant AR, on the other hand, should be considered a therapeutic target with respect to certain symptoms in SBMA patients.

Acknowledgements

We wish to thank Dr Yasushi Iwasaki and Mrs Sugiko Yokoi for technical assistance. This work was supported by a Center of Excellence (COE) grant from the Ministry of Education, Culture, Sports, Science, and Technology of Japan, and grants from the Ministry of Health, Labor, and Welfare of Japan.

References

Adachi H, Kume A, Li M, Nakagomi Y, Niwa H, Do J, et al. Transgenic mice with an expanded CAG repeat controlled by the human AR promoter show polyglutamine nuclear inclusions and neuronal dysfunction without neuronal cell death. Hum Mol Genet 2001; 10: 1039–48.

Adachi H, Katsuno M, Minamiyama M, Sang C, Pagoulatos G, Angelidis C, et al. Heat shock protein 70 chaperone overexpression ameliorates phenotypes of the spinal and bulbar muscular atrophy transgenic mouse model by reducing nuclear-localized mutant androgen receptor protein. J Neurosci 2003; 23: 2203–11.

Arbizu T, Santamaria J, Gomez JM, Quilez A, Serra JP. A family with adult spinal and bulbar muscular atrophy, X-linked inheritance and associated testicular failure. J Neurol Sci 1983; 59: 371–82.

Bates G. Huntingtin aggregation and toxicity in Huntington's disease. Lancet 2003; 361: 1642–4.

Chevalier-Larsen ES, O'Brien CJ, Wang H, Jenkins SC, Holder L, Lieberman AP, et al. Castration restores function and neurofilament alterations of aged symptomatic males in a transgenic mouse model of spinal and bulbar muscular atrophy. J Neurosci 2004; 24: 4778–86.

Doyu M, Sobue G, Mukai E, Kachi T, Yasuda T, Mitsuma T, et al. Severity of X-linked recessive bulbospinal neuronopathy correlates with size of the tandem CAG repeat in androgen receptor gene. Ann Neurol 1992; 32: 707–10.

Garden GA, Libby RT, Fu YH, Kinoshita Y, Huang J, Possin DE, et al. Polyglutamine-expanded ataxin-7 promotes non-cell-autonomous Purkinje cell degeneration and displays proteolytic cleavage in ataxic transgenic mice. J Neurosci 2002; 22: 4897–905.

Huynh DP, Yang HT, Vakharia H, Nguyen D, Pulst SM. Expansion of the polyQ repeat in ataxin-2 alters its Golgi localization, disrupts the Golgi complex and causes cell death. Hum Mol Genet 2003; 12: 1485–96.

Igarashi S, Tanno Y, Onodera O, Yamazaki M, Sato S, Ishikawa A, et al. Strong correlation between the number of CAG repeats in androgen receptor genes and the clinical onset of features of spinal and bulbar muscular atrophy. Neurology 1992; 42: 2300–2.

Ishisaka R, Utsumi T, Yabuki M, Kanno T, Furuno T, Inoue M, et al. Activation of caspase-3-like protease by digitonin-treated lysosomes. FEBS Lett 1998; 435: 233–6.

Katsuno M, Adachi H, Kume A, Li M, Nakagomi Y, Niwa H, et al. Testosterone reduction prevents phenotypic expression in a transgenic mouse model of spinal and bulbar muscular atrophy. Neuron 2002; 35: 843–54.

Katsuno M, Adachi H, Doyu M, Minamiyama M, Sang C, Kobayashi Y, et al. Leuprorelin rescues polyglutamine-dependent phenotypes in a transgenic mouse model of spinal and bulbar muscular atrophy. Nat Med 2003; 9: 768–73.

Kegel KB, Kim M, Sapp E, McIntyre C, Castano JG, Aronin N, et al. Huntingtin expression stimulates endosomal-lysosomal activity, endosome tubulation and autophagy. J Neurosci 2000; 20: 7268–78.

Kennedy WR, Alter M, Sung JH. Progressive proximal spinal and bulbar muscular atrophy of late onset. A sex-linked recessive trait. Neurology 1968; 18: 671–80.

La Spada AR, Wilson EM, Lubahn DB, Harding AE, Fischbeck KH. Androgen receptor gene mutations in X-linked spinal and bulbar muscular atrophy. Nature 1991; 352: 77–9.

La Spada AR, Roling DB, Harding AE, Warner CL, Spiegel R, Hausmanowa-Petrusewicz I, et al. Meiotic stability and genotype–phenotype correlation of the trinucleotide repeat in X-linked spinal and bulbar muscular atrophy. Nat Genet 1992; 2: 301–4.

Li M, Sobue G, Doyu M, Mukai E, Hashizume Y, Mitsuma T. Primary sensory neurons in X-linked recessive bulbospinal neuropathy: histopathology and androgen receptor gene expression. Muscle Nerve 1995; 18: 301–8.

Li M, Miwa S, Kobayashi Y, Merry DE, Yamamoto M, Tanaka F, et al. Nuclear inclusions of the androgen receptor protein in spinal and bulbar muscular atrophy. Ann Neurol 1998a; 44: 249–54.

Li M, Nakagomi Y, Kobayashi Y, Merry DE, Tanaka F, Doyu M, et al. Nonneural nuclear inclusions of androgen receptor protein in spinal and bulbar muscular atrophy. Am J Pathol 1998b; 153: 695–701.

Lieberman AP, Harmison G, Strand AD, Olson JM, Fischbeck KH. Altered transcriptional regulation in cells expressing the expanded polyglutamine androgen receptor. Hum Mol Genet 2002; 11: 1967–76.

Lin CH, Tallaksen-Greene S, Chien WM, Cearley JA, Jackson WS, Crouse AB, et al. Neurological abnormalities in a knock-in mouse model of Huntington's disease. Hum Mol Genet 2001; 10: 137–44.

Mariotti C, Castellotti B, Pareyson D, Testa D, Eoli M, Antozzi C, et al. Phenotypic manifestations associated with CAG-repeat expansion in the androgen receptor gene in male patients and heterozygous females: a clinical and molecular study of 30 families. Neuromuscul Disord 2000; 10: 391–7.

McCampbell A, Taylor JP, Taye AA, Robitschek J, Li M, Walcott J, et al. CREB-binding protein sequestration by expanded polyglutamine. Hum Mol Genet 2000; 9: 2197–202.

McCampbell A, Taye AA, Whitty L, Penney E, Steffan JS, Fischbeck KH. Histone deacetylase inhibitors reduce polyglutamine toxicity. Proc Natl Acad Sci USA 2001; 98: 15179–84.

Michalik A, Van Broeckhoven C. Pathogenesis of polyglutamine disorders: aggregation revisited. Hum Mol Genet 2003; 12: R173–86.

Minamiyama M, Katsuno M, Adachi H, Waza M, Sang C, Kobayashi Y, et al. Sodium butyrate ameliorates phenotypic expression in a transgenic mouse model of spinal and bulbar muscular atrophy. Hum Mol Genet 2004; 13: 1183–92.

Pinto AD, Lang AE, Chen R. The cerebellothalamocortical pathway in essential tremor. Neurology 2003; 60: 1985–7.

Ravikumar B, Duden R, Rubinsztein DC. Aggregate-prone proteins with polyglutamine and polyalanine expansions are degraded by autophagy. Hum Mol Genet 2002; 11: 1107–17.

Ross CA. Polyglutamine pathogenesis: emergence of unifying mechanisms for Huntington's disease and related disorders. Neuron 2002; 35: 819–22.

Ross CA, Poirier MA, Wanker EE, Amzel M. Polyglutamine fibrillogenesis: the pathway unfolds. Proc Natl Acad Sci USA 2003; 100: 1–3.

Sapp E, Schwarz C, Chase K, Bhide PG, Young AB, Penney J, et al. Huntingtin localization in brains of normal and Huntington's disease patients. Ann Neurol 1997; 42: 604–12.

Schilling G, Wood JD, Duan K, Slunt HH, Gonzales V, Yamada M, et al. Nuclear accumulation of truncated atrophin-1 fragments in a transgenic mouse model of DRPLA. Neuron 1999; 24: 275–86.

Schmidt BJ, Greenberg CR, Allingham-Hawkins DJ, Spriggs EL. Expression of X-linked bulbospinal muscular atrophy (Kennedy disease) in two homozygous women. Neurology 2002; 59: 770–2.

Simeoni S, Mancini MA, Stenoien DL, Marcelli M, Weigel NL, Zanisi M, et al. Motoneuronal cell death is not correlated with aggregate formation of androgen receptors containing an elongated polyglutamine tract. Hum Mol Genet 2000; 9: 133–44.

Sobue G, Hashizume Y, Mukai E, Hirayama M, Mitsuma T, Takahashi A. X-linked recessive bulbospinal neuronopathy. A clinicopathological study. Brain 1989; 12: 209–32.

Sobue G, Doyu M, Kachi T, Yasuda T, Mukai E, Kumagai T, et al. Subclinical phenotypic expressions in heterozygous females of X-linked recessive bulbospinal neuronopathy. J Neurol Sci 1993; 117: 74–8.

Sperfeld AD, Karitzky J, Brummer D, Schreiber H, Haussler J, Ludolph AC, et al. X-linked bulbospinal neuronopathy: Kennedy disease. Arch Neurol 2002; 59: 1921–6.

Steffan JS, Bodai L, Pallos J, Poelman M, McCampbell A, Apostol BL, et al. Histone deacetylase inhibitors arrest polyglutamine-dependent neurodegeneration in Drosophila. Nature 2001; 413: 739–43.

Tanaka F, Doyu M, Ito Y, Matsumoto M, Mitsuma T, Abe K, et al. Founder effect in spinal and bulbar muscular atrophy (SBMA). Hum Mol Genet 1996; 5: 1253–7.

Tanaka F, Reeves MF, Ito Y, Matsumoto M, Li M, Miwa S, et al. Tissue-specific somatic mosaicism in spinal and bulbar muscular atrophy (SBMA) is dependent on CAG repeat length and androgen receptor gene expression level. Am J Hum Genet 1999; 65: 966–73.

Tanaka M, Morishima I, Akagi T, Hashikawa T, Nukina N. Intra- and intermolecular beta-plated sheet formation in glutamine-repeat inserted myoglobin as a model for polyglutamine diseases. J Biol Chem 2001; 276: 45470–5.

Tanaka M, Machida Y, Nishikawa Y, Akagi T, Hashikawa T, Fujisawa T, et al. Expansion of polyglutamine induces the formation of quasi-aggregate in the early stage of protein fibrillization. J Biol Chem 2003; 278: 34717–24.

Taylor JP, Tanaka F, Robitschek J, Sandoval CM, Taye A, Markovic-Plese S, et al. Aggresomes protect cells by enhancing the degradation of toxic polyglutamine-containing protein. Hum Mol Genet 2003; 12: 749–57.

Terao S, Sobue G, Hashizume Y, Li M, Inagaki T, Mitsuma T. Age-related changes in human spinal ventral horn cells with special reference to the loss of small neurons in the intermediate zone: a quantitative analysis. Acta Neuropathol (Berl) 1996; 92: 109–14.

Trottier Y, Lutz Y, Stevanin G, Imbert G, Devys D, Cancel G, et al. Polyglutamine expansion as a pathological epitope in Huntingtin's disease and four dominant cerebellar ataxias. Nature 1995; 378: 403–6.

Walcott JL, Merry DE. Ligand promotes intranuclear inclusions in a novel cell model of spinal and bulbar muscular atrophy. J Biol Chem 2002a; 277: 50855–9.

Walcott JL, Merry DE. Trinucleotide repeat disease. The androgen receptor in spinal and bulbar muscular atrophy. Vitam Horm 2002b; 65: 127–47.

Watase K, Weeber EJ, Xu B, Antalffy B, Yuva-Paylor L, Hashimoto K, et al. A long CAG repeat in the mouse Sca1 locus replicates SCA1 features and reveals the impact of protein solubility on selective neurodegeneration. Neuron 2002; 34: 905–19.

Yamada M, Wood JD, Shimohata T, Hayashi S, Tsuji S, Ross CA, et al. Widespread occurrence of intranuclear atrophin-1 accumulation in the central nervous system neurons of patients with dentatorubral-pallidoluysian atrophy. Ann Neurol 2001a; 49: 14–23.

Yamada M, Hayashi S, Tsuji S, Takahashi H. Involvement of the cerebral cortex and autonomic ganglia in Machado–Joseph disease. Acta Neuropathol (Berl) 2001b; 101: 140–4.

Yamada M, Sato T, Tsuji S, Takahashi H. Oligodendrocytic polyglutamine pathology in dentatorubral-pallidoluysian atrophy. Ann Neurol 2002a; 52: 670–4.

Yamada M, Tsuji S, Takahashi H. Involvement of lysosomes in the pathogenesis of CAG repeat diseases. Ann Neurol 2002b; 52: 498–503.

Yoo SY, Pennesi ME, Weeber EJ, Xu B, Atkinson R, Chen S, et al. SCA7 knock in mice model human SCA7 and reveal gradual accumulation of mutant ataxin-7 in neurons and abnormalities in short-term plasticity. Neuron 2003; 37: 383–401.

Yvert G, Lindenberg KS, Picaud S, Landwehrmeyer GB, Sahel JA, Mandel JL. Expanded polyglutamines induce neurodegeneration and trans-neuronal alterations in cerebellum and retina of SCA7 transgenic mice. Hum Mol Genet 2000; 9: 2491–506.

Neuronal intranuclear hyaline inclusion disease showing motor-sensory and autonomic neuropathy

J. Sone, MD*; N. Hishikawa, MD*; H. Koike, MD; N. Hattori, MD; M. Hirayama, MD; M. Nagamatsu, MD; M. Yamamoto, MD; F. Tanaka, MD; M. Yoshida, MD; Y. Hashizume, MD; H. Imamura, MD; E. Yamada, MD; and G. Sobue, MD

Abstract—*Background:* Neuronal intranuclear hyaline inclusion disease (NIHID), a rare neurodegenerative disease in which eosinophilic intranuclear inclusions develop mainly in neurons, has not yet been described to present as hereditary motor-sensory and autonomic neuropathy. *Methods:* Patients in two NIHID families showing peripheral neuropathy were evaluated clinically, electrophysiologically, and histopathologically. *Results:* In both families, patients had severe muscle atrophy and weakness in limbs, limb girdle, and face; sensory impairment in the distal limbs; dysphagia, episodic intestinal pseudoobstruction with vomiting attacks; and urinary and fecal incontinence. No patients developed symptoms suggesting CNS involvement. Electrophysiologic study showed the reduced motor and sensory nerve conduction velocities and amplitudes, and also extensive denervation potentials. In sural nerve specimens, numbers of myelinated and unmyelinated fibers were decreased. In two autopsy cases, eosinophilic intranuclear inclusions were widespread, particularly in sympathetic and myenteric ganglion neurons, dorsal root ganglion neurons, and spinal motor neurons. These neurons also were decreased in number. *Conclusion:* Patients with neuronal intranuclear hyaline inclusion disease (NIHID) can manifest symptoms limited to those of peripheral neuropathy. NIHID therefore is part of the differential diagnosis of hereditary motor-sensory neuropathy associated with autonomic symptoms. Intranuclear hyaline inclusions in Schwann cells and in the myenteric plexus may permit antemortem diagnosis of NIHID.

NEUROLOGY 2005;65:1538–1543

Neuronal intranuclear hyaline inclusion disease (NIHID) is a rare neurodegenerative disease characterized by eosinophilic hyaline intranuclear inclusions in neurons of the central and peripheral nervous systems, associated with varying degrees of neuronal loss.[1-27] Etiology and pathogenesis remain unknown; a few patients show familial occurrence with mostly autosomal dominant inheritance.[2,3,6,15,19,23,24] Clinical manifestations of NIHID are highly variable, and can include cerebellar ataxia, dementia or mental retardation, pyramidal and extrapyramidal symptoms, generalized convulsion, and autonomic dysfunction. As a result, NIHID has been diagnosed as juvenile parkinsonism,[12,13,21] Friedreich ataxia variant,[3,4,8,9] multiple system atrophy,[5] and intestinal pseudoobstruction.[2,9,15,24]

Peripheral neuropathy symptoms rarely have been described except for certain forms of autonomic dysfunction such as gastrointestinal obstruction.[2,9,15,24] Muscle weakness and atrophy have been described only anecdotally in a few case reports as concomitant symptoms.[8,9,19,27]

Here we report two families affected by NIHID showing a similar peripheral neuropathy characterized by severe muscle atrophy in the limbs, limb girdles, and face; dysphagia; sensory impairment; and severe autonomic derangement, particularly gastrointestinal pseudoobstruction and bladder dysfunction. In affected patients of both families, the clinical diagnosis was hereditary motor and sensory neuropathy with autonomic failure.

Case reports. *Family 1.* Patient II-1. The proband was a 67-year-old man referred to our hospital because of gait disturbance. His brothers, sister, son, nephews, and niece also had gait disturbance (figure 1). When the patient was 32 years old, a gastric ulcer was treated with partial gastrectomy. Three years later, he was treated for appendicitis. At 65 years, he was found to have bilateral cataracts and corneal calcification.

Lower limb weakness, first noted at 30 years, had progressed gradually. The patient developed dysphagia and anorexia at 50 years old, associated with progressive weight loss; walking unaided was becoming difficult. He lost consciousness while bathing, and he noted difficulty in urination and subsequent incontinence. He had had an episode of hiccups, vomiting, and abdominal pain that continued for a few days after a car ride. Similar hiccups and vomiting recurred in association with urinary tract infection.

On neurologic examination, severe widespread muscle atrophy was evident in the face, upper and lower limbs, limb girdles, and

*Both authors contributed equally to this study.

From the Department of Neurology (Drs. Sone, Hishikawa, Koike, Hattori, Hirayama, Nagamatsu, Yamamoto, Tanaka, and Sobue), Nagoya University Graduate School of Medicine; the Department of Neuropathology, Institute for Medical Sciences of Aging (Drs. Yoshida and Hashizume), Aichi Medical University; and the Departments of Neurology (Dr. Imamura) and Pathology (Dr. Yamada), Hikone Municipal Hospital, Japan.

Disclosure: The authors report no conflicts of interest..

Received April 22, 2005. Accepted in final form August 1, 2005.

Address correspondence and reprint requests to Dr. Gen Sobue, Department of Neurology, Nagoya University Graduate School of Medicine, Nagoya 466-8550, Japan; e-mail: sobueg@med.nagoya-u.ac.jp

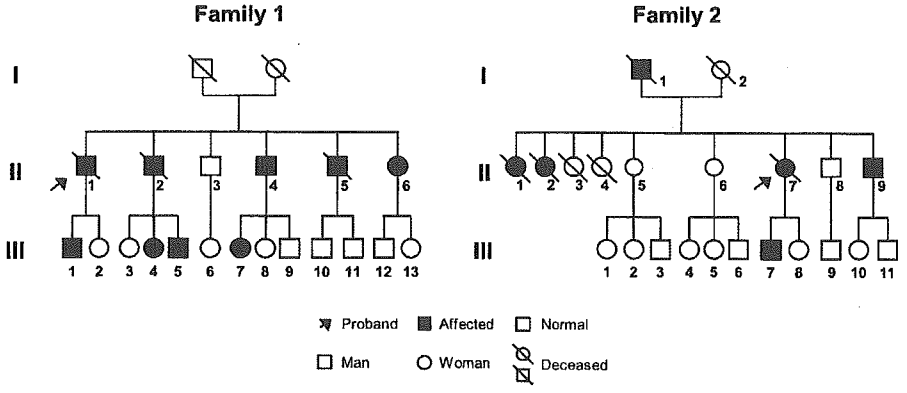

Figure 1. Pedigrees for the reported families with peripheral nervous system symptoms caused by neuronal intranuclear hyaline inclusion disease.

trunk (table 1). Fasciculations were not seen. Bilateral facial muscle weakness was observed in frontalis, orbicularis oculi, and orbicularis oris muscles. Weakness of the limbs was diffuse, and deep tendon reflexes were extensively diminished. Sensory impairment demonstrated in all modalities was seen predominantly in the distal limbs. No pathologic reflexes were observed. Foot deformity like pes cavus and hammer toe was not present. Laboratory results were normal, including serum creatine kinase and thyroid hormone concentrations. The CSF protein concentration was 65 mg/dL, without pleocytosis. The brain MRI showed mild brain atrophy. Leukoencephalopathy was absent. Nerve conduction study showed reduction of both motor and sensory nerve conduction velocity and amplitude, and prolongation of distal latency (table 2). Conduction block and temporal dispersion of compound muscle action potentials were not observed. On EMG, high amplitude potentials, positive sharp waves, and decreased interference patterns were widely spread. A cystometrogram showed an abdominal pressure pattern, indicating neurogenic bladder of atonic type. Orthostatic hypotension was not seen in a head-up tilt test, while a noradrenaline infusion test using a 3-μg dose raised the systolic blood pressure by 27 mm Hg, indicating supersensitivity to noradrenaline resulting from peripheral sympathetic nerve damage.

Sural nerve biopsy was performed, and pathologic assessment of the specimen was carried out as described previously[28-30] (figure 2A, table 3). Reduction of myelinated fiber density affected both small myelinated fibers and large myelinated fibers, especially the former. Thinly myelinated fibers, assessed as sheath thickness relative to axonal diameter, were abundant. Axonal sprouting was not conspicuous. Onion-bulb formation was not apparent. Unmyelinated fibers showed more severe reduction in number than myelinated fibers. Segmental remyelination, indicating fibers with relatively thin myelin sheaths, were frequent in teased-fiber preparations. Axonal degeneration was only slight. Intranuclear hyaline inclusions were found in Schwann cell.

No mutation was observed in *PMP22*, P0, Cx-32, transthyretin, SCA 1, SCA 2, SCA 3, SCA 6, and DRPLA genes. The patient died of suffocation when he was 70 years old, and autopsy was performed.

Other patients in Family 1. Clinical manifestations in other patients in Family 1 are summarized in table 1. Some patients had a past history of gastrointestinal disease such as gastritis or appendicitis (Patients II-4 and II-5). Age at symptom onset ranged from the first to third decade. The first symptom was gait disturbance or lower limb weakness. Muscle weakness and atrophy progressed and extended to involve the upper limbs, trunk, and face. The most severely affected patient (Patient II-4) showed nearly complete flaccid paralysis. Fasciculations could be seen in some patients (Patients II-4, III-1, and III-5). No one showed foot deformity. In most patients, autonomic dysfunction such as dysuria, constipation, and fecal incontinence was the next most prominent symptom. Episodes of vomiting occurred in Patients II-1, II-4, II-5, and II-6, including attacks that continued for several days after a car ride. In Patient II-6, electrogastrography showed an arrhythmic pattern of gastric motility after oral food intake. Frequency of gastric motility was much greater than the basic rhythm of three

Table 1 *Clinical manifestations in patients from two families*

Family, patient	Age, y/ sex	Onset, y	Motor: Muscle atrophy weakness L	LG	F	Fasciculation	Sensory: Superficial	Deep	Paresthesia	Autonomic: GI paralysis	Vomiting	Constipation	Bladder dysfunction	OH	Bulbar signs, dysphagia
Family 1															
II-1	67/M	30	++	++	+	–	+	+	–	–	+	–	+	–	+
II-4	59/M	16	++	++	++	+	++	++	–	+	+	+	+	–	+
II-6	53/F	30	+	+	+	–	+	+	–	+	+	+	+	–	–
III-1	37/M	20	+	+	–	+	+	+	–	–	–	–	+	–	–
III-4	36/F	30	+	+	–	–	–	–	–	–	–	–	–	–	–
III-5	34/M	26	+	+	–	+	–	–	–	–	–	–	–	–	–
Family 2															
II-7	48/F	26	+	++	+	+	+	+	+	+	–	+	+	–	+
II-9	41/M	ND	+	+	–	ND	ND	ND	ND	ND	ND	ND	ND	ND	ND

For motor and sensory impairments, – = not impaired; + = moderately impaired; ++ = severely impaired.

For autonomic dysfunction and bulbar signs, – = not impaired; + = impaired.

L = limbs; LG = limb girdle; F = facial muscles; GI = gastrointestinal; OH = orthostatic hypotension; ND = not determined.

Table 2 Electrophysiologic findings

Family, patient	Nerve conduction												
	Motor						Sensory						
	Median			Tibial			Median		Sural		Needle EMG		
	MCV, m/s	DL, ms	Amp, mV	MCV, m/s	DL, ms	Amp, mV	SCV, m/s	Amp, μV	SCV, m/s	Amp, μV	HA	PS	DI
Family 1													
II-1	38	4.6	4.1	26	8.0	5.2	37	8.4	25	3.9	+	+	+
II-4	NE	NE	NE	NE	NE	NE	NE	NE	NE	NE	ND	ND	ND
II-6	44	4.0	1.9	36	5.7	3.3	47	2.1	NE	NE	ND	ND	ND
III-1	41	ND	ND	ND	ND	ND	44	ND	ND	ND	ND	ND	ND
Family 2													
II-7	42.8	ND	ND	31.3	ND	ND	45.5	ND	30.1	ND	+	+	+
Controls (mean ± SD)	57.8 ± 3.7	3.4 ± 0.4	10.7 ± 3.5	46.9 ± 3.5	4.5 ± 0.8	10.9 ± 3.8	57.8 ± 4.7	23.5 ± 8.4	51.0 ± 5.1	11.5 ± 4.7			

Control values (mean ± SD) are based on a previously published report for n = 191(median), n = 121 (tibial), and n = 133 (sural).[28]

MCV = motor nerve conduction velocity; DL = distal latency; Amp = amplitude; SCV = sensory nerve conduction velocity; HA = high amplitude; PS = positive sharp waves; DI = decreased interference pattern; NE = not elicited; ND = not determined; + = positive findings.

contractions/minute; amplitude also was increased. Mild distal sensory impairment was demonstrated in the limbs; some patients were unaware of any sensory deficit. Laboratory examination showed mild elevation of serum creatine kinase in some patients (298 to1,403 IU/L). Nerve conduction study indicated the presence of motor dominant motor-sensory polyneuropathy (see table 2).

Family 2. Patient II-7. The 48-year-old female proband had no past medical history. Family history indicated that her father, brother, sisters, and son were affected (see figure 1).

At 26 years of age, she noted fatigue during a walk and difficulty standing on tiptoe. Four years later, she was unable to walk for more than 5 minutes because of leg muscle weakness. She came to notice dorsal numbness affecting both feet and weakness of both hands, as well as fasciculations in the thigh and arm. When she was 35 years old, muscle weakness and numbness had extended to the upper limbs. Difficulty was noted in climbing up stairs and riding a bicycle. Subsequently, she could not squat and rise unaided. At the age of 44 years, facial weakness and nasal voice developed. Chronic constipation sometimes progressed to ileus.

On neurologic examination at age 48, severe muscle weakness was observed in the neck, shoulder girdle, arms, and fingers, pelvic girdle, legs, and feet (see table 1). Muscle atrophy was diffuse but most prominent in the shoulder girdle and pelvic girdle. She could not walk or stand by herself. Facial muscle atrophy and weakness was accompanied by fasciculations. Nasality of the voice, dysarthria, and dysphagia were observed. Deep tendon reflexes were diffusely absent. All sensory modalities showed disturbance that was most prominent in the distal limbs. Mild reduction of both motor and sensory nerve conduction velocity was demonstrated electrophysiologically, as were prominent positive sharp waves and giant motor units (see table 2). Conduction block and temporal dispersion of compound muscle action potentials were not observed. Pes cavus and hammer toe was not seen. She presented an atonic bladder.

A sural nerve biopsy specimen revealed predominantly small-fiber loss, as had been found in Case 1. Thinly myelinated fibers also were present, although these were less conspicuous than in Case 1. Teased-fiber preparations revealed increased frequency of fibers showing segmental remyelination (see figure 2B, table 3). Intranuclear inclusions were demonstrated in Schwann cells (see figure 2C).

The patient died of sepsis at age 48 years. Autopsy was performed.

Other patients in Family 2. The proband's father (Patient I-1) was emaciated and showed weakness of the lower limbs. Her sisters (Patients II-1 and II-2) had muscle atrophy and ultimately could not walk before they died. Her brother (Patient II-9) was emaciated, and high-amplitude motor units were observed by EMG. Her son (Patient III-7) fell and tired easily. Both the proband's father (Patient I-1) and son (Patient III-7) were considered to be affected.

Findings at autopsy. Brains and spinal cords appeared macroscopically normal in both patients (Family 1, II-1 and Family 2, II-7) except that spinal roots were atrophic in Patient II-1 (Family 1). Microscopically, eosinophilic intranuclear inclusions were widely present in neurons as well as glial cells (figure 3, A and B). In neurons the intranuclear inclusions usually were round or oval, ranging in diameter from 3 to 10 μm. Some inclusions were surrounded by a pale halo. Occasionally two or more inclusions were present in one nucleus. Immunohistochemical investigation was

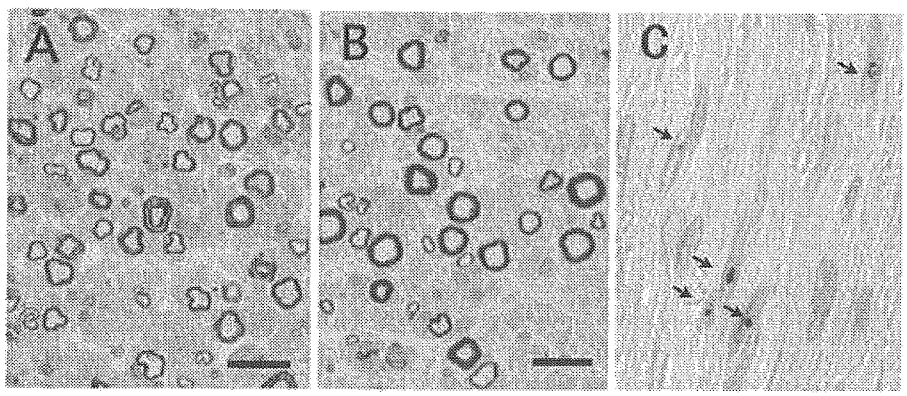

Figure 2. (A, B) Transverse section of a sural nerve biopsy specimen from Patient II-1 (Family 1, A) and from Patient II-7 (Family 2, B). Myelinated fibers, especially those of small diameter fibers, are decreased (scale bar = 20 μm). (C) Ubiquitin-immunoreactive intranuclear inclusions in Schwann cells of sural nerve (Patient II-7, Family 2).

Table 3 *Sural nerve histopathologic findings*

Pathology	Family 1, Patient II-1	Family 2, Patient II-7	Controls, n = 9
Myelinated fiber density, n/mm^2			
Total	3,569	3,550	8,190 ± 511
Large fiber	2,173	1,601	3,068 ± 294
Small fiber	1,396	1,949	5,122 ± 438
Unmyelinated fiber density, n/mm^2	9,082	11,404	29,913 ± 3457
Sprouting, n/mm^2	55	70	–
Teased fiber, %			
Segmental de/remyelination	49.2	31.1	9.5 ± 8.8
Axonal degeneration	3.0	5.4	1.7 ± 1.4
Schwann cell intranuclear inclusions	++	+	–

Control values (mean ± SD) are based on previously published reports.[29,30]

performed using a standard avidin-biotin-peroxidase complex method as previously described.[31] Most of the neuronal intranuclear inclusions were immunoreactive with anti-ubiquitin antibody (polyclonal, DAKO, 1:400), particularly along their peripheral rim (figure 3C). The inclusions showed no Congo-red staining and no immunostaining for α-synuclein (polyclonal, Santa Cruz, 1:400), phosphorylated tau (AT-8; monoclonal, Innogenetics, 1:1000), neurofilaments (monoclonal, DAKO, 1:200), expanded polyglutamine tract (1C2; monoclonal, Chemicon, 1:1000), or heat shock protein 70 (Hsp70; monoclonal, Stressgen, 1:100). Intranuclear inclusions also were present in glial cells. These glial inclusions usually were smaller than the neuronal inclusions, while showing similar staining features. By electron microscopic examination, the inclusion bodies consisted of haphazard meshwork of fine, straight filaments ranging from 12 to 16 nm in diameter (figure 3, G and H).

Tissue distribution and frequency of intranuclear inclusions were assessed by ubiquitin immunostaining, showing a similar distribution pattern in both patients. These were present not only in neural but also non-neural visceral tissues (figure 3, A through C, E, F). In neural tissues these inclusions were present in both the central and peripheral nervous system. In both patients inclusions were particularly common in sympathetic, sensory, and myenteric ganglion neurons, at a frequency of 70% in Patient II-7 (Family 1) and 41% in Patient II-1 (Family 2) in sympathetic ganglion neurons, 62% in sensory neurons in Patient II-7 (Family 2), and 70% or more in myenteric ganglion neurons in both patients (see figure 3E). Inclusions also were frequent in spinal motor neurons, the thalamus, putamen, locus ceruleus, brainstem cranial nerve nuclei, and Clarke's column; less frequently, these were present in the cerebral cortex, cerebellar cortex, and underlying white matter. Inclusions frequently were seen in peripheral nerve Schwann cell nuclei in both patients (see figure 2C). In contrast to widespread occurrence of neuronal and glial nuclear inclusions, neuronal loss and gliosis were restricted to sympathetic and sensory ganglion neurons, as well as spinal and brainstem motor neurons in both patients. There was no apparent neuronal loss in the cerebral cortex, thalamus, hypothalamus, caudate nucleus, putamen, Purkinje cells, dentate nucleus, substantia nigra, inferior olives, dorsal vagal nucleus, and other cranial nerve nucleus. The posterior column of the spinal cord showed loss of axons, with corresponding pallor upon myelin staining (see figure 3D).

We also found widespread but regionally selective occurrence of intranuclear inclusions in non-neural visceral tissues. Inclusions were present in parenchymal cells of the gut (see figure 3F), cardiac muscle, adrenal grand, lung, kidney, bladder, ovary, and other organs to a variable extent but not in skeletal muscles.

Discussion. Clinical abnormalities in patients of both families reported here were characterized as muscle atrophy and weakness in the proximal and distal limb muscles and limb girdles, associated with fasciculations, facial muscle atrophy, and dysphagia; sensory impairment affecting superficial and deep modalities, mainly in the distal portions of limbs; episodic intestinal pseudoobstruction symptoms with vomiting attacks; and urinary and fecal incontinence. While these fully developed symptoms were seen in advanced patients of both families, only muscle atrophy and weakness, and occasionally sensory symptoms, were observed in patients in the early phase of disease. Thus, motor and sensory symptoms apparently were the initial manifestations in these two families. No patients developed convulsions, personality change, dementia, cerebellar ataxia, or involuntary movements that would suggest CNS involvement. These features were similar among the patients of both families. Accordingly affected patients in both families were diagnosed with hereditary motor and sensory neuropathy including autonomic failure. Advanced patients presented a clinical picture somewhat similar to that seen in familial amyloid polyneuropathy. EMG and nerve conduction studies, as well as findings in sural nerve specimens, confirmed peripheral nerve involvement in these patients.

While previous reports of patients with NIHID have not described conspicuous peripheral neuropathy symptoms as in our present two families, several reports have noted the presence of peripheral nerve damage, mostly evident as needle EMG findings including chronic denervation potentials and nerve conduction findings of slowing.[2,4-10,12-15,19,21,24,27] However, nerve conduction was relatively well preserved in most patients in spite of EMG evidence of chronic denervation[5-7,14,24,27]; this suggested axonal impairment predominating over demyelination. Muscle atrophy and hyporeflexia also have been reported previously in some patients.[2-4,9,12,27] Sensory symptoms have attracted attention less frequently, although varying degrees of dorsal column fiber loss in the spinal cord have been observed in many autopsy cases.[3,4,6-9,11,12] The pathologic evidence suggests that peripheral sensory involvement probably is typical despite a paucity of sensory symptoms in most reported patients.

NIHID previously has been described as a disease involving the central rather than peripheral nervous system, since most patients reported so far have shown mainly CNS symptoms except for intestinal pseudoobstruction and some other autonomic manifestations.[2,9,15,24,27] Taking into account reported electrophysiologic and pathologic findings suggesting peripheral nerve involvement, peripheral nerve damage may be more widely present in NIHID than so far believed.

Among autonomic symptoms, urinary and fecal incontinence as well as gastrointestinal dysfunction presenting as intestinal pseudoobstruction have been described in NIHID.[2,15,17,24,27] Rectal biopsy spec-